

MONITORING SV40 LARGE T ANTIGEN HELICASE ACTIVITY USING
SURFACE PLASMON RESONANCE

THESIS

Presented to the Graduate Council of
Texas State University-San Marcos
in Partial Fulfillment
of the Requirements

for the Degree

Master of SCIENCE

by

Jason R Plyler, B.S.

San Marcos, Texas
August 2009

COPYRIGHT

by

Jason R Plyler

2009

ACKNOWLEDGEMENTS

I would like to thank all of my committee members, especially Wendi David, for all of their help and guidance. This research would not have been possible without their help. Also, I would like to thank the Welch Foundation for a summer Graduate Research Fellowship administered by the Department of Chemistry and Biochemistry at Texas State University-San Marcos. This allowed for continuous research activities that greatly influenced the amount of data collected. Finally, I would like to thank Texas State University-San Marcos for the opportunity and facilities to conduct a Master's Thesis.

TABLE OF CONTENTS

	Page
ACKNOWLEDGEMENTS	iv
LIST OF TABLES.....	vi
LIST OF FIGURES.....	vii
CHAPTER	
I. INTRODUCTION.....	1
II. METHODS AND MATERIALS	18
III. RESULTS AND DISCUSSION.....	30
APPENDIX.....	59
REFERENCES.....	62

LIST OF TABLES

Table	Page
1. DNA SEQUENCES	20
2. SUMMARY OF CONTACT TIME AND SALT OPTIMIZATION ASSAYS.....	45
3. INHIBITION OF T-AG DUPLEX HELICASE ACTIVITY BY TMPYP4, TEL11, AND DISTAMYCIN	50

LIST OF FIGURES

Figure	Page
1. SV40 LARGE T ANTIGEN (T-AG) DODECAMER AT THE ORIGIN OF REPLICATION (OR).....	3
2. THE FOUR MAJOR PROTEIN DOMAINS OF SV40 LARGE T ANTIGEN.....	4
3. TOPOLOGY OF G-QUADRUPLEX DNA.....	6
4. THREE SMALL MOLECULE INHIBITORS OF HELICASE ACTIVITY.....	8
5. GENERAL THEORY OF SURFACE PLASMON RESONANCE (SPR) ANALYSIS.....	12
6. SPR ANALYSIS OF T-AG DUPLEX HELICASE ACTIVITY AND INHIBITION.	14
7. STRATEGY FOR QUADRUPLEX DNA UNWINDING ASSAY.....	17
8. T-AG BINDING TO 5' IMMOBILIZED TAG DNA1.....	32
9. ATP DEPENDENCE FOR T-AG BINDING TO IMMOBILIZED TAG DNA1.....	34
10. T-AG BINDING TO TAG DNA1 WITHOUT ATP, IN THE PRESENCE OF GAMMA-S-ATP, AND WITH ATP..	36
11. SSB AS A REPORTER FOR G4 DNA UNWINDING.....	38
12. T-AG DUPLEX HELICASE ACTIVITY IN THE PRESENCE OF ATP AND GAMMA-S-ATP..	40
13. DUPLEX SUBSTRATE UNWINDING AND RE-FORMATION.....	40

14. DETERMINATION OF T-AG CONCENTRATION TO REMOVE ~90% OF COMPLIMENTARY DUPLEX STRAND (TAG DNA2).....	42
15. SALT OPTIMIZATION ASSAY FOR T-AG DUPLEX HELICASE ACTIVITY.....	43
16. OPTIMAL CONTACT TIME FOR T-AG HELICASE ACTIVITY.....	44
17. TMPYP4 INHIBITION OF T-AG DUPLEX HELICASE ACTIVITY.....	47
18. TEL 11 INHIBITION OF T-AG DUPLEX HELICASE ACTIVITY.....	48
19. DISTAMYCIN A INHIBITION OF T-AG DUPLEX HELICASE ACTIVITY.....	49
20. T-AG BINDING TO THE SV40 ORIGIN OF REPLICATION SEQUENCE.....	52
21. T-AG BINDING TO THE PARTIAL SV40 ORIGIN OF REPLICATION SEQUENCE.....	53
22. T-AG BINDING TO TAG DNA1/TAGCOMPG4 COMPLEX WITHOUT ATP, IN THE PRESENCE OF GAMMA-S-ATP, AND WITH ATP.....	56
23. T-AG BINDING AND UNWINDING OF TAG1:TAGCOMPG4.....	57

CHAPTER I

INTRODUCTION

In order to better understand the way that eukaryotes perform DNA replication, repair and recombination, scientists often use less complex systems as genetic and mechanistic models. Simian virus (SV) 40 is an excellent model for eukaryotic replication due to similarities in the way it replicates DNA, as well as its defined genome and proteins (1). SV40 commandeers host proteins to replicate its genome but does produce several essential proteins, including large T antigen (T-ag), a multifunctional protein required for viral replication and transformation (1).

1. SV40 Large T Antigen

Upon first entering the cell, the viral coat or capsid of SV40 is shed and the genomic DNA of the virus enters the nucleus of the cell. This event triggers early transcription and SV40 messenger RNA (mRNA) is transcribed by the host RNA polymerase and eventually exported to the cytoplasm. The exported mRNA molecule that codes for the large T-ag protein is then translated by the host cell ribosome. Active T-ag re-enters the nucleus where it performs two major functions: 1) It binds specific SV40 viral DNA called the origin of replication (OR)

containing the pentanucleotide repeat, GAGGC (2), stimulating DNA synthesis, and 2) It binds newly replicated viral DNA stimulating late transcription. During late transcription, viral proteins (VP) 1, 2, and 3 are formed to produce new capsids for virus DNA enclosure and transport out of the cell (3).

In the presence of ATP and Mg^{2+} , T-ag assembles as a double-hexamer on the viral OR and stimulates replication by unwinding the SV40 genome in a 3'-5', bi-directional manner (4) (Figure 1). The OR contains a 64-bp core origin, which is composed of three separate regions: the central region or site II, a 27-bp perfect palindrome with four GAGGC pentanucleotides; an adenine:thymine rich region upstream of site II; and an imperfect palindromic (EP) sequence downstream of site II (3, 4). The pentanucleotides of site II are arranged as inverted pairs with the complementary sequence CTCCG. When a T-ag monomer binds the pentanucleotide sequence, several protein-protein interactions follow, resulting in the addition of five T-ag monomers to the first (5, 6) Alternatively, hexamers that are already formed in solution may contact the origin of replication and bind simultaneously (5). Once a dimer of hexamers is formed, it possesses bi-directional helicase activity. The EP region of the OR is the site for initial unwinding (7), and helicase activity is then "jump-started" at the AT region (presumably since less energy is required to 'melt' AT base pairs, compared to GC base pairs) (7). Furthermore, a series of eight adenines have been reported in the AT rich region, which induces a small bend in the DNA that may facilitate melting of the DNA as T-ag begins to translocate 3'-5' down the template (8).

OR (11). Residues 266-627 fold into the region of the protein containing helicase activity. In fact the helicase region contains three distinct domains; a zinc domain comprising the first eighty residues (266-345), the AAA+ module (ATPase associated with diverse cellular activities extended family) (residues 415-548) responsible for ATP hydrolysis and binding (12), and a globular domain formed from residues 346-414 and 549-627. The AAA+ module is a common motif for all helicases in SF3, and is found in many protein-DNA remodeling proteins (13). The remaining C-terminal region (residues 628-708) is theorized to help in viral assembly and in determining the host-range (14) (Figure 2).

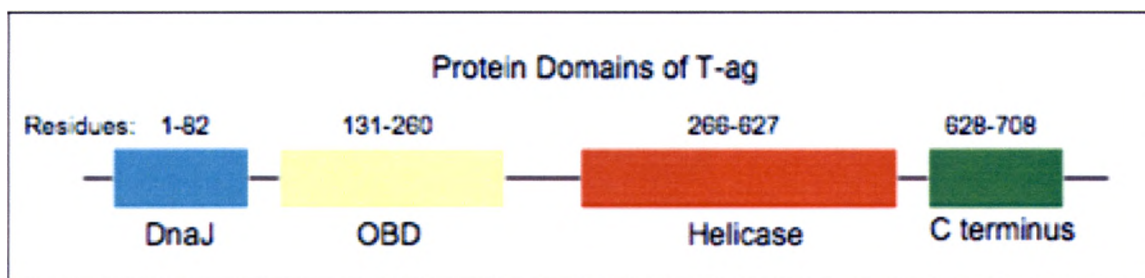


Figure 2. The four major protein domains of SV40 Large T Antigen. The DnaJ domain (light blue, amino acid residues: 1-82) helps promote cell growth of infected cells. The OBD domain (tan, amino acid residues: 131-260) is the region of the protein that recognizes the SV40 origin of replication (OR). The Helicase domain (red, amino acid residues: 266-627) folds into the non-specific DNA unwinding portion of the protein. The C terminus domain (amino acid residues: 628-708) is thought to help in viral assembly.

2. G-quadruplex Helicase Activity of T-ag

As described, T-ag is essential for initiating replication of the SV40 virus *in vivo*. T-ag also unwinds synthetic oligonucleotide substrates, and much of the work performed to characterize and investigate T-ag helicase activity has been accomplished employing forked duplex DNA substrates containing a free 3'-end (15). A single T-ag hexamer is sufficient to unwind synthetic substrates *in vitro*. In addition to duplex unwinding, T-ag has been shown to unwind synthetic quadruplex DNA substrates (16). The significance of T-ag quadruplex helicase activity is unknown, although the SV40 genome does possess nucleotide sequences that may form into quadruplex DNA regions (17).

Quadruplex DNA forms from guanine (G) rich regions of DNA, through the assembly of Hoogsteen base-paired guanine residues at the four corners of a central tetrad (Figure 3). G-quadruplex DNA results from one, two, or four strands of DNA, giving unimolecular (G₄'¹), bimolecular (G₄'²), or tetramolecular (G₄) structures, respectively (Figure 3).

SV40 T-ag is not the only helicase to possess G-quadruplex unwinding activity. Members of a large family of highly conserved DNA helicases, called the RecQ family (named for the original helicase found in *E. coli*), also unwind quadruplex DNA (18). Members of this family include yeast Sgs1p (19) and two human homologs: BLM (20), and WRN (21). These RecQ helicases possess a conserved G₄ binding region, which is not present in T-ag (22). The importance of this G-quadruplex helicase activity is not known, but patients with Bloom's and

Werner's syndromes have mutations in the *blm*, and *wrn* genes leading to inactive helicase proteins (23). Both Bloom's and Werner's syndromes have individual clinical manifestations, but patients with dysfunctional proteins share a dramatic predisposition to cancer (23).

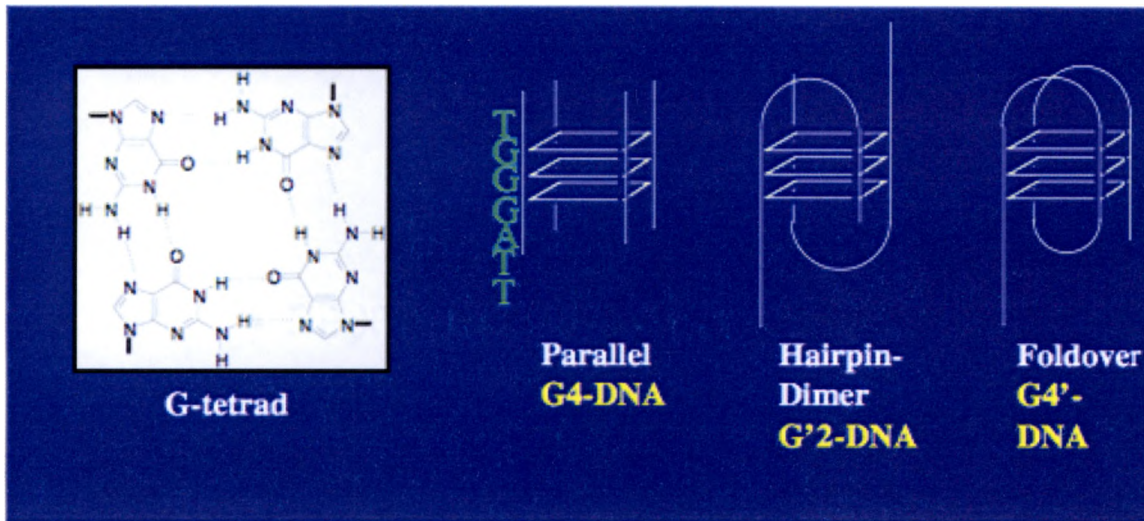


Figure 3. Topology of G-quadruplex DNA. On the left is a top-view of four guanines forming a G-tetrad through eight Hoogsten hydrogen bonds (shown as dashed lines). Shown on the right are three G-quadruplex structure topologies. The first is composed of four separate strands of DNA (sequence TTAGGG, green) and is the parallel tetramolecular, G4 topology. The second is composed of two separate strands of DNA, and is called the hairpin-dimer or bimolecular G'2 topology, and on the far right the fold-over or unimolecular quadruplex G4' topology is composed of a single strand of DNA.

One hypothesis is that G-quadruplex regions of DNA are regulatory sequences that may control access to DNA, such as during transcription or replication. Efficient unwinding of these regions by G-quadruplex helicases such as T-ag would then be necessary before replication could proceed. Up to 370,000 potential stretches of human genomic DNA capable of forming quadruplex structures (24) have been identified computationally; however, to

date only one instance has been observed of quadruplex structures *in vivo* (in *E. coli*) (25). However, evidence is accumulating that quadruplex DNA formation may be important in promoter regions (26) of oncogenes such as p53 or c-myc and in recombination sequences, such as immunoglobulin switch regions (27). Recently, FANCD1 helicase has been demonstrated to unwind various quadruplex DNA topologies, presumably in its role maintaining chromosomal stability, although its ability to unwind unimolecular quadruplexes was not determined. (28).

Quadruplex DNA may also form in the sequences that are found in the end regions of the chromosomes, called telomeres. This is due to the fact that telomeres have a very high concentration of G-rich nucleotide repeats (29). In humans, this repeat sequence is TTAGGG and these G residues may potentially form quadruplex structures (30).

Telomere maintenance in most cancer cells is accomplished with telomerase, an enzyme that is not expressed in most somatic cells (31). Telomerase is responsible for extending the single-stranded G-rich overhang region of telomeres, the shortening of which is associated with a finite number of normal cellular replication events (31). Inhibition of telomerase is consequently a potential chemotherapeutic strategy.

G-quadruplex stabilizing small molecules have been demonstrated to inhibit telomerase *in vivo* (32) and many of these same compounds also interfere with G-quadruplex helicases, although the mode of inhibition may be different. For instance, the cationic porphyrin 5, 10, 15, 20-Tetra(*N*-methyl-4-pyridyl)

porphine (TMPyP4) (Figure 4) inhibits RecQ G-quadruplex helicase activity and T-ag duplex helicase activity, although to a different extent in each case (33).

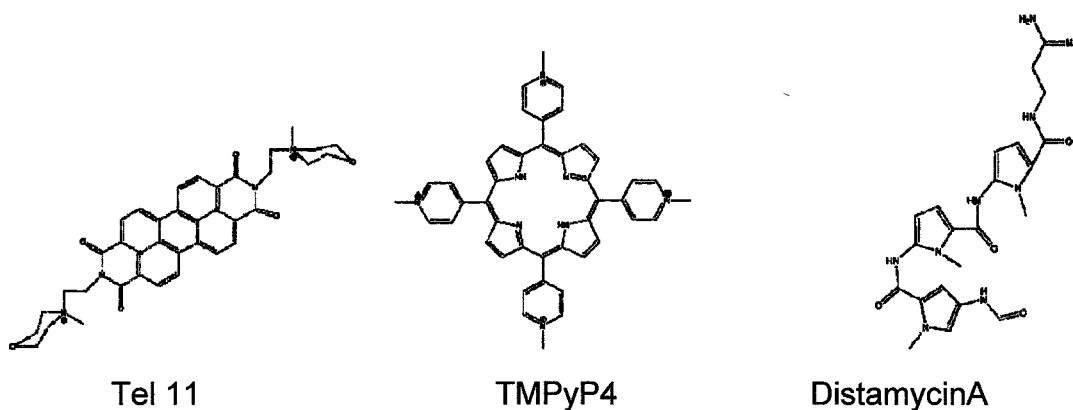


Figure 4. Three small molecule inhibitors of helicase activity. TMPyP4 is a cationic porphyrin that forms stacking interactions with DNA bases in duplex and G-quadruplex DNA. Distamycin A binds to the minor groove of duplex DNA, and interacts with G-quadruplex DNA. Tel 11 is a perylene diimide that forms stacking interactions with DNA, binding with high affinity to G-quadruplex DNA.

Investigation of the effects of small molecules that interact with quadruplex DNA and interfere with quadruplex-processing enzymes may lead to potential therapeutic strategies in other situations as well. As mentioned above, quadruplex DNA formation in the promoter region of c-myc may regulate access to the promoter (34). When the G-quartet region is stable the oncogene functions normally, but if the G-quartet is unwound the oncogene is aberrantly over-expressed leading to possible tumorigenesis. Inhibiting the unwinding of G-quadruplex DNA formed at oncogenic promoters could lead to decreased transcription and thus decreased cell growth (34).

The selectivity of small molecules for G-quadruplex DNA *versus* other DNA topologies, as well as selectivity for particular G-quadruplex processing

proteins are both important issues to be addressed, especially because the two types of selectivity do not necessarily correlate. For instance, TMPyP4 binds G-quadruplex DNA, with a stoichiometry of 2 porphyrins per quadruplex structure (35), but also binds duplex DNA to some extent. Although TMPyP4 inhibits telomerase, the quadruplex unwinding activity of the RecQ helicases and T-ag duplex helicase activity, it does not inhibit T-ag quadruplex helicase activity to any great extent (18, 36, 37, and 38). Tel 11 (Figure 4) is a perylene diimide designed to form stacking interactions with quadruplex DNA (17). Tel 11 has a higher affinity for quadruplex DNA *versus* duplex DNA due to stacking interactions on the faces of the terminal G-quartets (22, and 39) and at high concentrations (~100 μ M) Tel 11 can completely prevent T-ag G-quadruplex helicase activity (17). Distamycin A (Figure 4) binds to the minor groove of duplex DNA and binds G-quadruplex DNA through interactions with the grooves and by stacking on the terminal faces of the quartets (36, and 40). Research has shown that Distamycin A blocks BLM duplex unwinding but not G-quadruplex helicase activity (41), and recently Distamycin A was in fact shown to weakly inhibit T-ag quadruplex unwinding activity (17). It is clear that binding mode alone is not predictive of helicase inhibition.

3. Analysis of Helicase Activity

Most helicase assays employ polyacrylamide gel electrophoresis (PAGE) analysis of the unwinding of radiolabeled DNA substrates in order to determine activity. This method works well for analyzing unwinding of duplex and intermolecular quadruplex substrates but it is difficult to discern unwinding of G4' quadruplex topologies, even with native PAGE. In addition, information concerning the mode of inhibition for small molecules is difficult to obtain with standard PAGE analysis. Förster resonance energy transfer (FRET) analysis with labeled DNA substrates can also yield information about unwinding of DNA substrates, including intramolecular quadruplex DNA (42), however, loading of the helicase under consideration onto the fluorescently labeled DNA may be problematic.

4. Project Goal

The main goal of this project was to develop a real-time assay of T-ag helicase activity and inhibition that would specifically improve our ability to monitor unwinding of unimolecular quadruplex DNA structures.

Surface plasmon resonance (SPR) is a label-free real time method for monitoring biomolecular interactions (43) and we believed an SPR-based assay of T-ag helicase activity would be advantageous for investigating intramolecular G-quadruplex unwinding. To begin with it was necessary to verify that T-ag binds to various DNA substrates (single-stranded DNA, duplex DNA, and G-

quadruplex DNA) under conditions for SPR experiments. Once these initial assays were performed, the focus shifted to the development and optimization of unwinding assays to monitor T-ag helicase activity and inhibition. Finally, an improved method for observing T-ag unwinding of an intramolecular G-quadruplex DNA substrate was developed.

5. Research Strategy

5.1 SPR Analysis

The SPR instrument is designed to detect very small variations of mass that are proportional to binding events at the molecular level. Detection relies on a change in the refractive index of polarized light that is reflected off of a glass-backed gold-coated sensor chip immobilized with a molecule of choice (Figure 5). Incoming light is polarized by a prism, which increases the wave vector of the light as it approaches the gold layer.

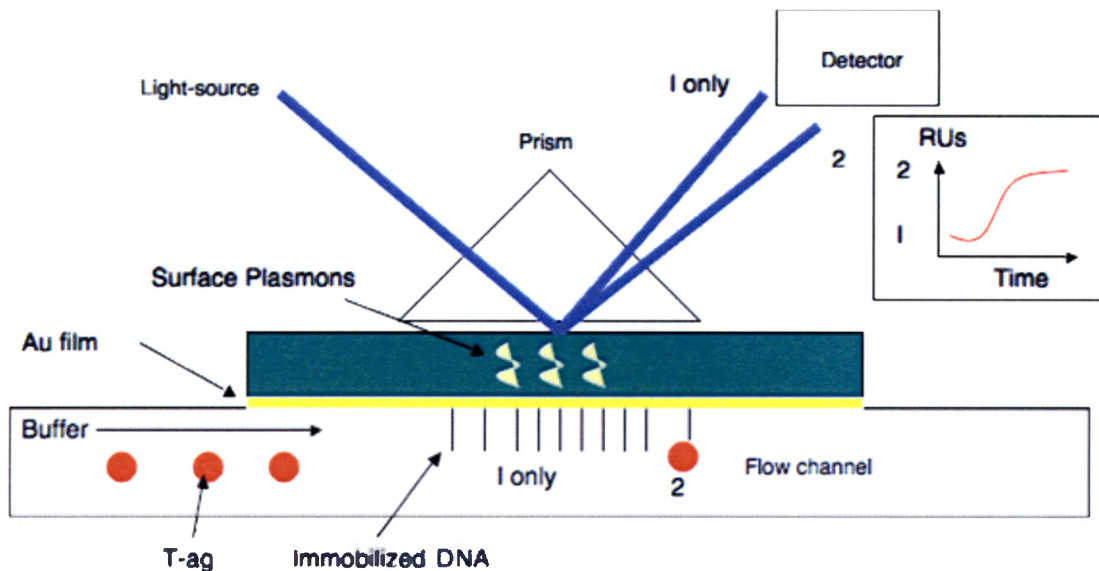


Figure 5. General Theory of Surface Plasmon Resonance (SPR) analysis. Immobilized DNA is suspended in the flow channel. Injected T-ag flows over the immobilized DNA (1 only) and interacts to form a complex (2). The relative amount of surface plasmons generated is proportional to the mass at the sensor surface; therefore the angle of refraction of the polarized light (blue line) changes between 1 only and 2. The detector records the intensity and angle of refraction and converts the signal into response units (RUs). A plot of the RUs vs. Time generates a sensorgram (inset graph), from which information concerning the real-time binding event is obtained.

Surface plasmons are surface electromagnetic waves that propagate from oscillations of electrons along a metal surface in the presence of a dielectric. The polarized light at the gold-coated glass surface acts as the dielectric to generate surface plasmons based on the mass bound to the gold matrix layer. If a complex is formed, the mass increases on the matrix layer and consequently the angle of refraction is changed and thus the binding event can be detected.

Our strategy involved immobilization of various DNA substrates on SPR sensor chips and subsequently injecting T-ag to observe binding and unwinding

events in real-time. Biotinylated DNA was immobilized to the sensor chips at a gold surface coated with a streptavidin-dextran matrix layer. The sensor chip is essentially a thin layer of glass with a 50 nm layer of gold, and a 100 nm “matrix” layer on top of the gold. Biotin forms a very tight non-covalent bond with streptavidin, with a K_D of 10^{-15} M (44). Formation of this strong bond essentially immobilizes DNA on the chip. After the DNA substrate was immobilized on the sensor chip, an association between T-ag and the DNA would result in an increase in RUs observed. If DNA is subsequently removed from the surface of the matrix layer (*i.e.* through unwinding activity), a corresponding decrease in RUs would result, reflecting the amount removed.

5.2 T-ag/DNA substrate binding and optimization

Once the DNA was immobilized on the surface of the sensor chip, monitoring the actual binding and interaction of T-ag with the synthetic DNA was necessary. Also, the other various *in vitro* requirements of T-ag helicase activity required verification with SPR before any other work could be accomplished. This included testing requirements for ATP, Mg^{2+} , and a free 3' tail of DNA (not a blunt-ended DNA substrate), for T-ag proper function. After verification of conditions for T-ag activity, experiments focused on monitoring duplex, and quadruplex DNA unwinding and inhibition.

The development and optimization of a duplex DNA unwinding assay was performed. The initial step required forming a duplex on the sensor chip surface between two semi-complimentary oligonucleotides (Figure 6). T-ag could then

be injected to determine if it bound and unwound the duplex, thereby removing one of the oligonucleotides from the sensor chip (Figure 6).

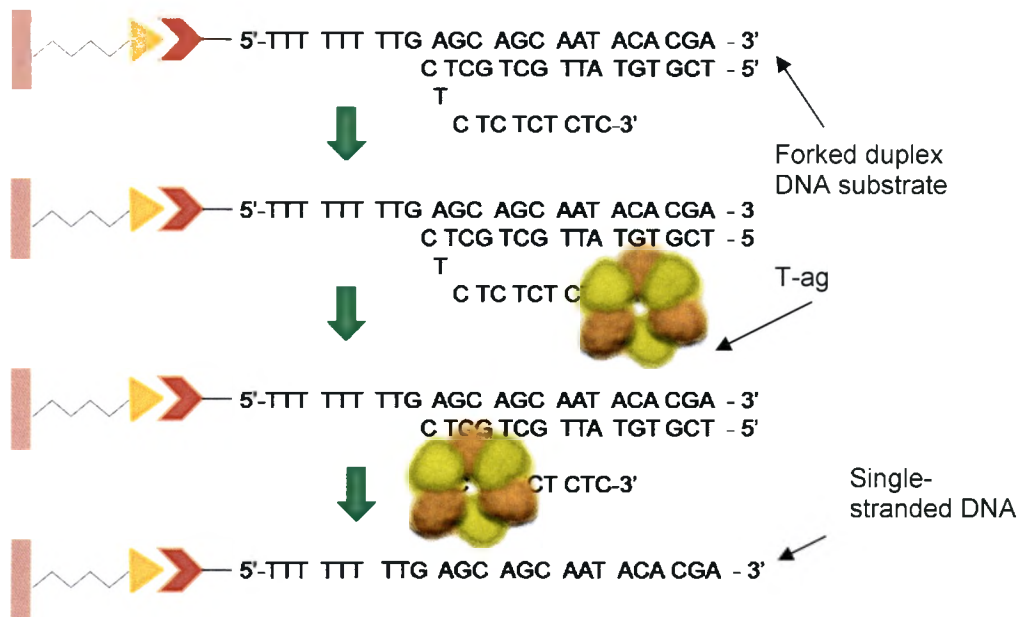


Figure 6. SPR analysis of T-ag duplex helicase activity and inhibition.

Biotinylated single-stranded DNA is immobilized on the surface of a streptavidin-coated gold sensor chip (SA chip, GE Healthcare). Injecting a partially complementary strand of DNA onto the immobilized DNA forms a forked duplex substrate containing a free 3' -tail. T-ag (yellow and orange hexamer) binds to the free 3'-tail and translocates in a 3'-5' direction, unwinding the duplex DNA, leaving only single-stranded immobilized DNA.

Once the T-ag unwinding event was observed by SPR, there were many experimental factors that had to be optimized in the development of this assay. The optimization assays included testing a range of salt and ATP concentrations, various protein-DNA contact times, and minimum T-ag concentration necessary for ample unwinding of the duplex. Once a reliable and optimized duplex unwinding assay was established for T-ag, further hypotheses could be tested.

5.3 Analysis of T-ag duplex helicase activity and its inhibition

Another area of the project was to test the effect of small molecule DNA binding agents on T-ag helicase activity. The mode of inhibition is not necessarily apparent using traditional PAGE assays of helicase activity. For instance, whether the small molecule directly inhibits the helicase or must first form a complex with the DNA substrate to interfere with helicase activity is a question that is difficult to answer with PAGE analysis. The benefit of SPR-based analysis of helicase activity is especially evident in this situation due to the real-time nature of the assay. Since SPR-based observation of helicase activity occurs in real-time it is possible to determine whether a DNA/drug complex is required for inhibition of activity.

Comparing duplex helicase inhibition *versus* quadruplex helicase inhibition is important for addressing selectivity issues. TMPyP4, Tel 11, and Distamycin A, potential inhibitors of T-ag unimolecular quadruplex helicase activity, were investigated for their ability to inhibit the duplex helicase activity of T-ag. This will allow for T-ag quadruplex helicase inhibition with the same molecules to be tested in the future.

5.4 Development of an improved quadruplex unwinding assay

Previous research has shown that T-ag does indeed unwind an intramolecular quadruplex 5'-(TTT GGG)₄TT-3' (45). Initial experiments in this project focused on repeating previous experiments with single-stranded binding protein (SSB) and TMPyP4 as reporter agents in assays testing the ability of T-

ag to unwind G-quadruplex structures. A newly designed and more direct assay for monitoring quadruplex unwinding was developed that doesn't require the use of a reporter molecule. The strategy shown in Figure 7 was employed. The same initial immobilized DNA strand as shown in Figure 6 was used, but the complimentary oligonucleotide was much longer and possessed an intramolecular-quadruplex-forming sequence. The DNA substrate had a free 3' tail available, but T-ag would be forced to unwind the intramolecular quadruplex structure prior to unwinding the duplex region, in order to remove the complimentary strand of DNA from the sensor chip.

6. Summary

A reliable, real-time assay of T-ag helicase activity and inhibition was developed for duplex DNA and unimolecular quadruplex DNA structures. To begin with it was necessary to verify using SPR that T-ag binds to various DNA substrates and once these initial assays were performed, the focus was turned to the optimization of unwinding assays to monitor T-ag helicase activity and inhibition. Finally, an improved method for observing T-ag unwinding of an intramolecular G-quadruplex DNA substrate was developed.

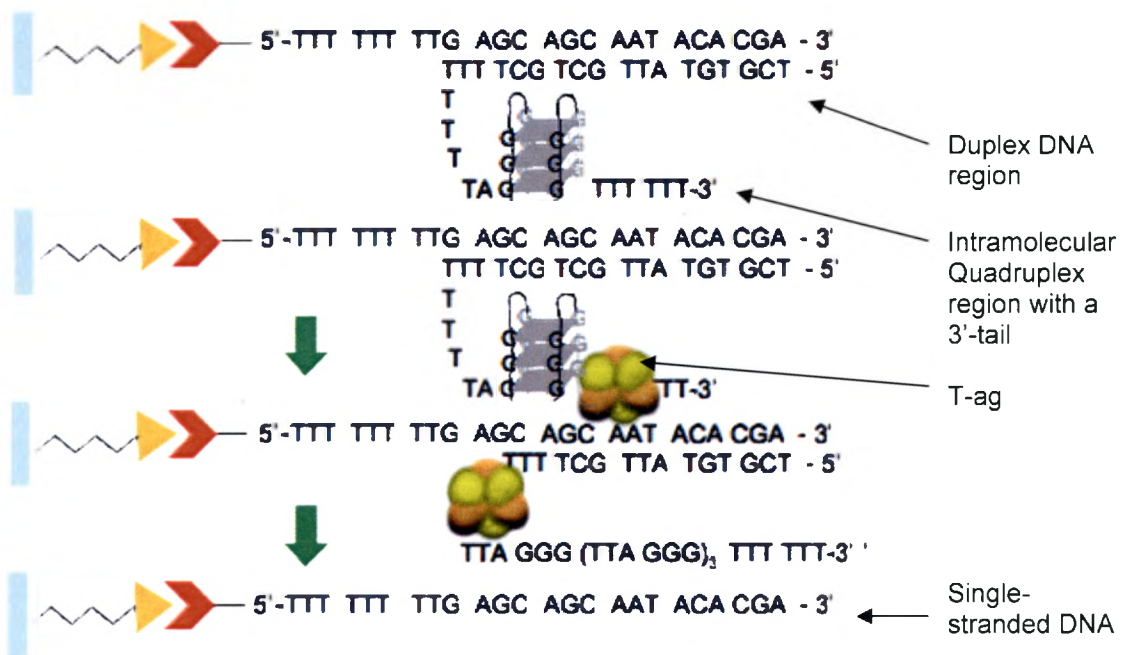


Figure 7. Strategy for quadruplex DNA unwinding assay. Biotinylated single-stranded DNA is immobilized on the surface of a streptavidin-coated gold sensor chip (SA chip, GE Healthcare). Injecting a partially complementary strand of DNA onto the immobilized DNA forms a partial duplex DNA substrate with a G4' unimolecular quadruplex-forming region (in the presence of 150 mM K⁺) followed by a free 3' -tail. T-ag (yellow and orange hexamer) binds to the free 3'-tail and translocates in a 3'-5' direction, unwinding the intramolecular quadruplex region prior to the duplex DNA, leaving only single-stranded immobilized DNA.

CHAPTER II

MATERIALS AND METHODS

1. Chemicals and Reagents

All reagents for buffer solutions were obtained from Sigma-Aldrich (St. Louis, MO) or GE Healthcare (Piscataway, NJ), unless otherwise noted. Working stock solutions were made with **HBS-EP buffer** (0.01 M HEPES, pH 7.4, 0.15 M NaCl, 3 mM EDTA, and 0.005% v/v P20 surfactant), **HBS-EP-Mg²⁺ Buffer** (0.01 M HEPES, pH 7.4, 0.15 M NaCl, 3 mM EDTA, 10 mM MgCl₂, and 0.005% v/v P20 surfactant), or **HBS-EP-K⁺ Buffer** (0.01 M HEPES, pH 7.4, 0.15 M KCl, 3 mM EDTA, and 0.005% v/v P20 surfactant). Minor modifications to these buffer stock solutions were made on occasion and are noted in the individual methods. Potassium chloride and magnesium chloride were obtained from EM Science (Gibbstown, NJ). All buffers were degassed and passed through 0.2 mm filters (Nalgene) prior to use. Degassing was accomplished by leaving the buffer under vacuum for a minimum of 10 minutes after filtration. DNA sequences were obtained from Integrated DNA Technologies (Coralville, IA). Biotinylated sequences were HPLC purified; additional sequences were either PAGE purified or desalted and used without further purification. The DNA sequences tabulated

in Table 1 were used and will be hereafter referred to according to the monikers in **bold font**.

SV40 T-ag was obtained from CHIMERx, where it was isolated from cultured insect cells and stored in 10 mM Tris-HCl, pH 8.0, 100 mM NaCl, 1.0 mM EDTA, 1.0 mM dithiothreitol, and 50% (v/v) glycerol. T-ag (aliquot 1: 1.3 $\mu\text{g}/\mu\text{L}$, aliquot 2: 1.9 $\mu\text{g}/\mu\text{L}$) was used without further purification. Aliquots of the T-ag enzyme were stored at -80°C and diluted with HBS-EP- Mg^{2+} buffer to the desired concentrations just prior to use.

The small molecules TMPyP4 [5, 10, 15, 20-tetra(*N*-methyl-4-pyridyl) porphine] and Distamycin A used for inhibitor studies were obtained from Sigma-Aldrich. Tel 11 was a gift from Dr. Sean Kerwin at The University of Texas at Austin (Austin, TX).

Surface plasmon resonance experiments were performed using a BiacoreX instrument and streptavidin-derivatized (SA) sensor chips (GE Healthcare). During the course of an SPR experiment as an analyte binds to a ligand immobilized on the gold surface of the sensor chip, a change in the refractive index at the gold surface is detected during the binding event. This change in refractive index is converted into a response unit (RU) that correlates to the magnitude of binding.

Table 1. DNA sequences. Sequences containing a 5'-BioTEG linker were immobilized on SA sensor chips.

DNA	Sequence (green sequences are complimentary to the preceding red sequence)
Human Telomeric G4 DNA	5'-BioTEG-(TTAGGG) ₄ TT-3'
TAG DNA1	5'-BioTEG-TTTTTTTT GAGCAGCAATACACGA -3'
TAG DNA2	3'-CTCTCTCTCTCT CGTCGTTATGTGCT -5'
compG4	3'-TTTT(GGGATT) ₄ CCCGTTATGTGCT -5'
TAGcompG4	3'-(T) ₆ (GGGATT) ₄ (T) ₆ TCGTCGTTATGTGCT -5'
TAG-OBD	5'-BioTEG-TGA GCT ATT CCA GAA GTA GTG- TAATTTTTTTTTATTTATGCAGAGGCCGAGGCCGCCTC- GGCCTCTGAGCTATTCCAGAAGTAGTG -3'
Fragment A	3'-ATTAAAAAAATAAATACGTCTCCGGCTCCGGCGGA- GCCGGAGACTCGATAAGGTCTTCATCAC-5'
Fragment C	3'-TCCGGTTCAG- ATAAATACGTCTCCGGCTCCGGCGGA- GCCGGAGACTCGATAAGGTCTTCATCAC-5'
ODNA	5'-BioTEG- GCTCAGAGGCCGAGGCCGCCTCGGCC -3'
ODNAcomp1	3'- CGAGTCTCCGGCTCCGCCGGAGCCGG -5'
ODNAcomp2	3'-TTTTACTCCGGCTCCGCCGGAGCCGG-5'

2. Single-stranded DNA experiments

2.1 T-ag binding to immobilized single-stranded DNA

SA sensor chips were preconditioned with three short injections of 1 M NaCl/ 50 mM NaOH prior to DNA immobilization. Biotinylated DNA dissolved in HBS-EP buffer (10 -100 nM) in 10 μ L increments was injected over a single flow cell at 5 μ L/min until the desired immobilization level was achieved (~200 – 900 RU). Since 1000 RU corresponds to 1 ng of material immobilized on the gold

surface, the amount of DNA immobilized on the chip was calculated from the observed RU following immobilization. In all cases, unless otherwise noted, the remaining flow cell of the sensor chip was left blank for use as a reference cell.

SV40 T-ag was prepared at nanomolar hexamer concentrations in HBS-EP-Mg²⁺ buffer. Just prior to injection an excess of ATP (~40 mM, or concentration otherwise noted) was added to the T-ag solution and 100 μ L aliquots were injected at a constant flow rate (5 – 30 mL/min) using the normal inject mode. Dissociation times after the injection varied, depending on the observed dissociation characteristics, but were typically 120 – 180 seconds. Longer dissociation times were employed for T-ag binding to TAG DNA1. Regeneration of the sensor chip surface was usually accomplished with 0.005% SDS, with the exception of the inhibitor assays. A more potent regeneration solution was required to remove the small molecules from the DNA after each injection. A solution of 2 M guanidine-HCl, 10 % (v/v) formamide, and 0.3 % (v/v) p20 surfactant (Sigma-Aldrich) was dissolved in distilled H₂O and used for all inhibition assays directly after injecting T-ag. Injections of T-ag without ATP added or with gamma-S-ATP (~ 5 mM) instead of ATP were performed for comparison to the response observed in the presence of ATP. In addition, the effect of including ATP in the running buffer (HBS-EP-Mg²⁺) was investigated. ATP (5 mM) was added to the running buffer as well as the T-ag solution and dissociation was monitored for several minutes. All experiments were performed in multichannel mode using the non-immobilized flow cell as a reference cell to correct for nonspecific binding and bulk effects of the buffer solutions.

Binding kinetics were approximated to determine an equilibrium binding constant, K_D , for the T-ag/DNA interaction. From sensorgrams obtained for the binding of T-ag to immobilized DNA, rates of association (k_{on}) and dissociation (k_{off}) were obtained separately using BIAevaluation software supplied with the Biacore X instrument (GE Healthcare). These rates were used to calculate an approximate equilibrium response (Req), which was converted to the molar concentration of [T-ag hexamer-DNA] complex at equilibrium using the volume of the individual flow cells (~0.6 mL) and the fact that 1 RU corresponds to 1 pg of material at the sensor surface. Assuming equilibrium conditions for binding of single-stranded DNA by the T-ag hexamer, the following relationship approximates K_D for a 1:1 binding interaction:

$$k_{off}[\text{T-ag hexamer-DNA}] = k_{on}[\text{DNA}][\text{T-ag hexamer}]$$

$$K_D[\text{T-ag hexamer-DNA}] = [\text{DNA}][\text{T-ag hexamer}] \quad (\text{Eq. 1})$$

The molar concentration of the T-ag/DNA complex was determined as stated above and plotted *versus* the product of the molar concentration of immobilized DNA and the molar concentration of T-ag hexamer in the injections using Kaleidagraph to yield a linear relationship with a slope equal to K_D .

2.2 T-ag binding to immobilized intramolecular quadruplex sequence

Prior to immobilization of the 5'-biotinylated G4' DNA sequence, (TTAGGG)₄TT, SA sensor chips were preconditioned as before. The DNA was

immobilized in HBS-EP buffer (600 –1000 RU) and then folded into a quadruplex structure on the chip in HBS-EP-K⁺ buffer. The extent of folding was verified using *E. coli* single strand binding protein (SSB) (40). The maximum response, R_{\max} , that could be observed from SSB interacting with immobilized G4 DNA if it were 100% single-stranded was calculated using Equation 2:

$$R_{\max} = RU_{\text{im}} * (MW_A/MW_L) * S \quad (\text{Eq. 2})$$

where RU_{im} is the RU increase obtained after immobilization of G4 DNA, MW_A is the molecular weight of the SSB monomer, MW_L is the molecular weight of the immobilized G4 DNA, and S is equal to four due to the tetrameric nature of active SSB. Under the experimental conditions utilized here the sensor chips immobilized with G4 DNA were >95% folded into G-quartets in the presence of HBS-EP- K⁺ buffer.

T-ag injections were performed as described for single-stranded DNA experiments, both in the presence and absence of ATP. Rates of association (k_{on}) and dissociation (k_{off}) were obtained as before using BIAevaluation software supplied with the Biacore X instrument (GE Healthcare).

In order to determine whether or not the immobilized G4' DNA was unfolded after interaction with T-ag, SSB was used as a probe for the amount of unfolded, single-stranded DNA present on the sensor chip. The G4 DNA was first allowed to fold into an intramolecular quadruplex structure by flowing HBS-EP- K⁺ buffer over the sensor chip surface for fifteen minutes. The running buffer

was then changed to HBS-EP-Mg²⁺ buffer. SSB (30 μ L of 0.16 μ M) was injected, followed by 0.005% SDS (25 μ L) to remove any SSB that remained bound to the DNA. T-ag with ATP (100 μ L of 13.5 nM T-ag) was injected, followed by 0.005% SDS to remove any remaining T-ag. SSB was then injected again and the response was compared to the response obtained during the initial injection of SSB. The percent change in RU noted during binding of SSB to the DNA before and after T-ag injection was calculated. To ensure that the difference in response observed was not due to SSB or to the regeneration using SDS the procedure was replicated without the addition of T-ag.

3. Double-stranded DNA experiments

3.1 Preparation of duplex substrates

Formation of the duplex DNA substrates was accomplished on sensor chips immobilized with biotinylated single strand DNA sequences. Solutions of complementary DNA were dissolved in HBS-EP buffer (100 μ M) and injected in 50 μ L increments over the surface of flow cells (previously immobilized with biotinylated single-stranded DNA) at 5 μ L/min until complete hybridization was observed. The change in RU indicating maximum hybridization was calculated from Equation 2:

$$R_{\max} = RU_{\text{im}} * (MW_A/MW_L) * S \quad (\text{Eq. 2})$$

where R_{\max} is the response indicating 100% hybridization, RU_{im} is the RU increase obtained after immobilization of biotinylated single-stranded DNA, MW_A is the molecular weight of the complement DNA oligomer, and MW_L is the molecular weight of the immobilized single stranded DNA. The interaction between the two strands is a 1:1 binding interaction; therefore multiplication of the above R_{\max} value by a binding stoichiometry factor (S) is not necessary.

3.2 Monitoring and Optimizing T-ag duplex helicase activity

T-ag injections were performed as described above for binding to single-stranded DNA. At the end of the injections, T-ag and the DNA complementary strand were lost from the sensor chip. The percent duplex unwound was calculated by dividing the amount of complement removed from the chip (decrease in RU) by the original RU amount observed upon hybridization (R_{\max} , in most cases). Regeneration of the duplex substrate was accomplished simply by rehybridizing the complementary strand to the immobilized DNA substrate through further injections of complement. The same T-ag experiments were done without ATP or with gamma-S-ATP to compare the response observed.

The optimization assays included three main steps to complete. The first step was forming a duplex substrate on the sensor chip as described above. The R_{\max} value was then determined for this duplex and a series of T-ag injections were performed to determine what concentration of T-ag would generate approximately 90% unwound DNA substrate. This would allow for the highest concentration of T-ag to be used without going over 100% unwound substrate.

This was done in order to normalize results from different experiments. The following formulas were used to calculate % unwound, with the example calculations made with data from Figure 13:

$$\begin{aligned}
 R_{\max \text{ TAG2}} &= \text{RUs of immobilized TAG1} \times (\text{MW}_{\text{TAG2}}/\text{MW}_{\text{TAG1}}) \times (\text{TAG1}:\text{TAG2}) \\
 R_{\max \text{ TAG2}} &= 560 \text{ RUs} \times (7821 \text{ dal}/ 7911 \text{ dal}) \times 1/1 \\
 R_{\max \text{ TAG2}} &= 550 \text{ RUs}
 \end{aligned}
 \tag{Eq. 3}$$

$$\begin{aligned}
 \text{RU}_{\text{DIFF}} &= \text{RU}_{\text{final}} - \text{RU}_{\text{initial}} \\
 \text{RU}_{\text{DIFF}} &= 1600 \text{ RUs} - 1100 \text{ RUs} \\
 \text{RU}_{\text{DIFF}} &= 500 \text{ RUs}
 \end{aligned}
 \tag{Eq. 4}$$

$$\begin{aligned}
 \% \text{ Unwound} &= \text{RU}_{\text{DIFF}} / R_{\max \text{ TAG2}} \times 100\% \\
 \% \text{ Unwound} &= 500 \text{ RUs} / 550 \text{ RUs} \times 100\% \\
 \% \text{ Unwound} &= 91\%
 \end{aligned}
 \tag{Eq. 5}$$

Once the optimal T-ag concentration of 2.9 nM was determined (for the particular batch of T-ag), the next parameter to optimize was the NaCl concentration used throughout the assay. The HBS-EP-Mg²⁺ Buffer was made as described above except the concentration of NaCl was varied from the normal 150 mM. For the salt assay, four 1 L aliquots were made without any NaCl and then each was individually adjusted to arrive at the final concentrations of: 1.5 mM, 15 mM, 50 mM, and 300 mM NaCl. These four aliquots were then used as the running buffer for each individual salt assay and for all dilutions of ATP and T-ag that were used during each run. All other parameters were kept constant including a flow rate of 20 $\mu\text{L}/\text{min}$ as well as the total volume of T-ag injected (80 μL).

The last of the parameters to be optimized for the duplex unwinding assay was T-ag time dependence. We wanted to determine if changing the contact time of T-ag would affect the helicase activity on the duplex substrate. Based on

previous sensorgrams, five injection values were calculated that would yield a spread of contact times for T-ag. Using a constant flow of 20 $\mu\text{L}/\text{min}$ the volumes: 8, 17, 42, 67, and 75 μL , would give contact times: 25, 50, 125, 200, and 225 seconds, respectively, for T-ag flowing over the duplex substrate.

3.3 Inhibition of T-ag duplex helicase activity

Inhibition of T-ag duplex helicase activity was demonstrated using the small molecule inhibitors: TMPyP4, Distamycin A, and Tel 11. All three inhibitors were prepared identically to keep the assays as precise as possible and to allow side-by-side comparison of the results. Solutions of each inhibitor were dissolved in HBS-EP- Mg^{2+} buffer at various concentrations (500 nM – 10 mM) and were injected at 20 $\mu\text{L}/\text{min}$ for 180 seconds using the manual inject mode. Before complete dissociation of the small molecule from the DNA had occurred, a constant concentration of T-ag (9.7 nM) in HBS-EP- Mg^{2+} buffer containing ATP was immediately injected at the same flow rate for 240 seconds, again using the manual inject function. After the end of the T-ag injection, the percent duplex unwound for each initial concentration of inhibitor was calculated. Additionally, TMPyP4 was added to the T-ag injection solution for 5 minutes prior to injection for one trial. Sensorgrams in which TMPyP4 was pre-incubated with T-ag were compared to sensorgrams in which TMPyP4 was allowed to interact with the duplex substrate prior to T-ag injection in order to determine whether an existing DNA/small molecule complex was necessary for inhibition to occur.

4. Improved T-ag quadruplex unwinding assay

TAG DNA 1 was immobilized on a new sensor chip as described above to begin the improved T-ag quadruplex unwinding assay. Instead of flowing TAG DNA2 over the surface to form a duplex substrate, two alternate complimentary oligonucleotides were obtained for this study: compG4 and TAGcompG4. The first, compG4, was complimentary to TAG DNA1 for the first eleven bases forming a short duplex, followed by the repeat sequence (TTAGGG)₄, capable of forming an intramolecular quadruplex region in the presence of K⁺, and finally a very short poly T 3'-tail for T-ag loading. TAGcompG4 was designed to form a longer duplex with TAG DNA1 of fourteen base-pairs, followed by a poly T spacer, then the human telomeric repeat (TTAGGG)₄, and finally a longer poly T 3'-tail. As it turned out, compG4 wouldn't bind to TAG DNA1 immobilized on the sensor chip. After TAGcompG4 bound to TAG DNA1, the running buffer was changed from HBS-EP-K⁺ Buffer (used to induce quadruplex formation) to HBS-EP-Mg²⁺ Buffer for T-ag helicase activity. Finally, injections of 2.9 nM T-ag with 40 mM ATP were flowed over the sensor chip and the percent DNA substrate unwound was calculated as before.

5. T-ag assay on SV40 origin of replication containing DNA

A pair of sensor chips was preconditioned and the biotinylated origin of replication containing DNA (TAG-OB and ODNA) was immobilized as described above. The major difference with these DNA substrates was that they are palindromic in nature. As described in Chapter I, the entire origin of replication is

a 64 base-pair sequence that contains four pentanucleotides (site II, Figure 1) that are perfect palindromes. This means that when the DNA is single-stranded it has a high propensity to fold back on itself and form secondary structures, most likely being small hairpin loops. This gives the oligonucleotides a very high T_m (70 –75°C) and makes it virtually impossible to add complimentary DNA to the sensor chip and form the duplex origin of replication. Therefore, the temperature of the Biacore was raised to 37 °C and the complimentary DNA was heated to 85 °C prior to injection. This allowed for a small amount of the complimentary DNA to bind and form a duplex that represented an *in vitro* version of the origin of replication. An aliquot of 2.9 nM T-ag was then injected immediately after this duplex was formed so that helicase activity could be observed. The percent unwound was calculated as described above.

CHAPTER III

RESULTS AND DISCUSSION

The major goal of this research was to develop a real-time assay of SV40 T-ag helicase activity and inhibition that would specifically improve the ability to monitor unwinding of unimolecular G4' quadruplex substrates. T-ag was observed to bind to various immobilized DNA substrates (single-stranded DNA, double-stranded or duplex DNA, and unimolecular G-quadruplex containing DNA) in the presence of ATP and Mg^{2+} . After binding of T-ag to various single-stranded DNA substrates was verified and determined to be ATP-dependant, the focus of the project turned to developing a duplex unwinding assay. Conditions for monitoring duplex helicase activity and inhibition by several small molecules were optimized. Finally, an improved quadruplex unwinding assay was developed and tested for future use.

1. Single-stranded DNA experiments

1.1 T-ag binding assays on immobilized TAG DNA1

A range of increasing T-ag concentrations (1.1 -20 nM) with 4 mM ATP and 10 mM Mg^{2+} were injected at 20 μ L/min over a streptavidin-coated sensor

chip derivatized with ~475 RUs of TAG DNA1 (Figure 8). The SV40 T-ag hexamer loads onto synthetic DNA substrates at the 3'-end and unwinds DNA in a 3'-5' direction (6). A much greater binding response would be expected for immobilized substrates possessing a free 3'-tail, compared to 3'-immobilized substrates. Therefore the main purpose was to show the direct relationship between injected T-ag concentration and relative protein binding on 5' immobilized DNA, which has a 3'-tail free in the flow cell. Previously, T-ag was demonstrated to bind to 3'-immobilized DNA as well, although the response was diminished and a slower flow rate (5 $\mu\text{L}/\text{min}$) and longer injection time were required. An equilibrium binding constant, K_D , of 0.54 μM ($R^2 = 0.9706$) was determined for this interaction between T-ag and the 3'-immobilized DNA, within the range of reported binding constants for T-ag to non-specific synthetic DNA substrates (45). As predicted, T-ag exhibited much greater binding to 5'-immobilized TAG DNA1 due to the fact that T-ag highly favors loading onto a free 3'-tail in solution. These results demonstrate that assembly of the T-ag hexamer was being observed in real-time. T-ag binds with a fast *on* rate and displays continuous binding throughout the injection time, in contrast to results obtained for binding of T-ag to 3'-immobilized single-stranded DNA. Consequently, binding could not be modeled as described in the experimental section, and an equilibrium constant for this interaction was not calculated. Also, a slow *off* rate was observed and with higher concentrations a proportional amount of T-ag remained bound to TAG DNA1 after the dissociation period. This is most likely

due to the fact that multiple T-ag hexamers are being loaded onto the TAG DNA1 substrate and disassembly at the end of the injection is relatively slow.

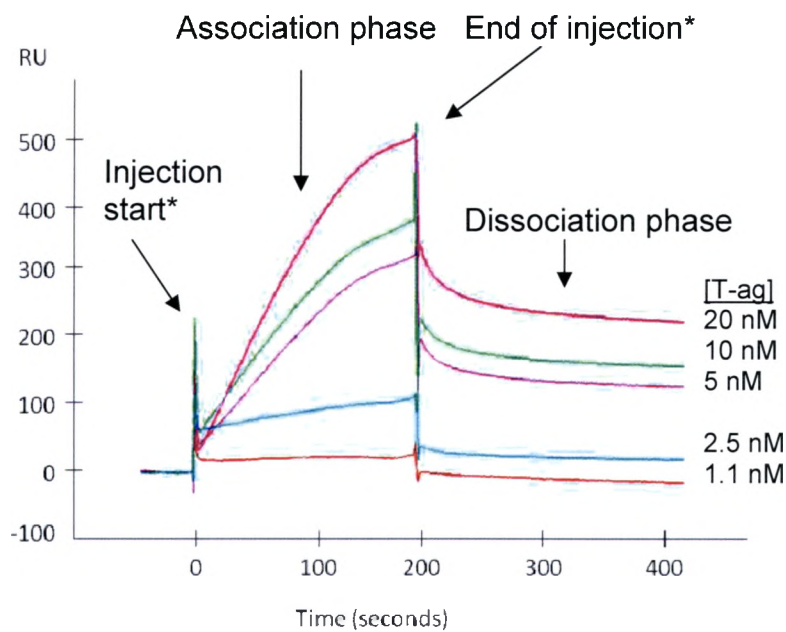


Figure 8. T-ag binding to 5' immobilized TAG DNA1. All injections of T-ag were 100 μ L performed at 30 μ L/min in the presence of 4 mM ATP and HBS-EP buffer containing 10 mM Mg^{2+} . T-ag binding at 1.1 nM (red trace), 2.5 nM (light blue trace), 5 nM (purple trace), 10 nM (green trace), and 20 nM (magenta trace) hexamer concentration, respectively. The amount of TAG DNA1 immobilized was \sim 475 RUs. Binding occurs with a quick on rate, and a slower off rate. It is likely that multiple hexamers bind each DNA substrate since the response never quite reaches equilibrium at higher T-ag hexamer concentrations. Each sensorgram trace is reference-subtracted to account for non-specific binding and bulk buffer effects. (*All reference subtracted sensorgrams in this section will have "Injection start" and "End of injection" spikes, due to a slight time delay between injection through both flow cells.)

In order to demonstrate that active T-ag hexamers were the species involved in binding the immobilized DNA substrates, ATP-dependence was investigated. First, the optimal amount of ATP required for T-ag binding to immobilized TAG DNA1 was determined. The ATP concentration in the

injections was varied, while keeping the T-ag and Mg^{2+} concentrations fixed at 2.9 nM and 10 mM, respectively. The previous sensor chip (~475 RUs of TAG DNA1) was used for this assay after regenerating the surface with 2 M guanine-HCl in water (described in Chapter II). T-ag was injected with ATP from 1 mM to 32 mM. As the ATP concentration increased, so did the observed binding of T-ag (Figure 9), until a concentration of 16 mM ATP, at which point an increase in ATP did not lead to increased binding of T-ag. This result supports the hypothesis described above that multiple hexamers can be loaded onto a 5'-immobilized DNA substrate with a free 3'-end. Even though the T-ag concentration is not increasing during the injections, more hexamers can be formed and translocate in the presence of adequate ATP present (45).

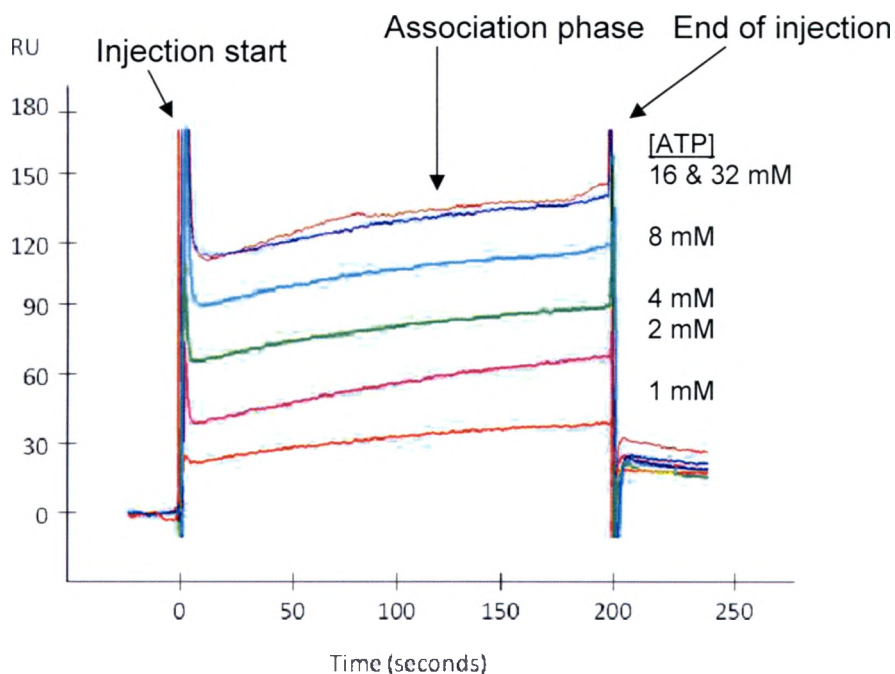


Figure 9. ATP dependence for T-ag binding to immobilized TAG DNA1.

Various concentrations of ATP were mixed with 2.9 nM T-ag in HBS-EP buffer with 10 mM Mg^{2+} to determine the effect of ATP on binding of T-ag to immobilized TAG DNA1 (~475 RUs). All T-ag injections were 100 μ L at a flow rate of 30 μ L/min. The observed binding at 1 mM (red trace), 2 mM (magenta trace), 4 mM (green trace), 8 mM (light blue trace), 16 mM (dark blue trace), and 32 mM (brown trace), ATP, respectively, is optimal at 16-32 mM ATP.

A slight increase of RUs is observed after the dissociation period at increased ATP concentrations (Figure 9). Based upon these results, the amount of ATP used in T-ag injections was maintained at 32-40 mM in subsequent experiments.

The binding of T-ag to immobilized TAG DNA1 was greatly decreased when gamma-S-ATP was used in place of ATP (Figure 10). The gamma phosphate bond of this ATP analogue cannot be hydrolyzed. Although formation of T-ag hexamers occur in the presence of gamma-S-ATP, translocation of T-ag along the DNA substrate is not possible. The results obtained for T-ag binding to

TAG DNA1 in the absence of ATP, presence of gamma-S-ATP, and presence of ATP are important to verify that ATP is required for the formation of hexamers and generation of free energy required for T-ag to translocate down the DNA substrate in a 3' to 5' direction. This corresponds to earlier reports that T-ag oligomerization is ATP-dependent (4). This also suggests that the hexamer cannot form without ATP or gamma-S-ATP present, which is reflected by the very low observed binding response in the absence of ATP. But T-ag does recognize the sugar-phosphate backbone of DNA in its monomer state and this is most likely the cause of the small amount of binding observed in the sensorgram. Although T-ag binds in the presence of gamma-S-ATP, translocation doesn't occur, preventing multiple hexamers from loading onto the DNA substrate. Therefore, the increased binding observed with ATP present is likely from loading of multiple hexamers onto the immobilized TAG DNA1.

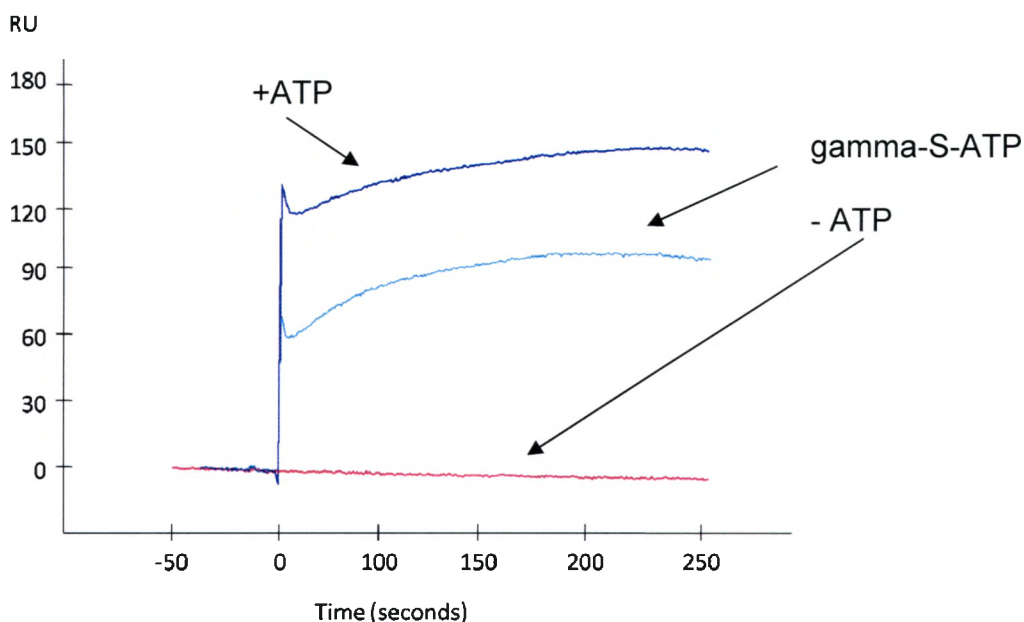


Figure 10. T-ag binding to TAG DNA1 without ATP, in the presence of gamma-S-ATP, and with ATP. T-ag (2.3 nM) was injected at 20 $\mu\text{L}/\text{min}$ in HBS-EP buffer with 10 mM Mg^{2+} in the absence of ATP (magenta trace), presence of 5 mM gamma-S-ATP (cyan trace), and presence of 5 mM ATP (blue trace). Multiple hexamers of T-ag could bind the DNA with normal ATP in the injection dilution, which is reflected by the increased RUs. The amount of TAG DNA1 immobilized was ~ 475 RUs. Data shown are for the DNA-containing flowcell only and is not reference-subtracted.

1.2 T-ag quadruplex unwinding assay with G4' DNA

After verifying the binding of the T-ag hexamer to immobilized single-stranded DNA, assays were performed to test whether T-ag unwinding of an unimolecular quadruplex could be observed using SPR. The human telomeric G4' DNA was immobilized to a final RU value of ~ 765 RUs. Single-stranded binding protein (SSB) from *E. coli* was used as the reporter molecule to determine if the DNA was in its single-stranded form or folded into a quadruplex structure. The G4' DNA was induced to fold into a quadruplex structure prior to

the initial injection of SSB with HBS-EP K⁺ buffer (150 mM K⁺), and calculated to be >95% folded (described in Chapter II). The binding response for SSB (12 μg/mL for both injections) was greatly increased after T-ag was injected over the immobilized G4 DNA (Figure 11), indicating a decrease in the amount of folded quadruplex. Control experiments in the absence of T-ag injections showed no increase in SSB binding, suggesting that SSB and the experimental conditions alone do not lead to an increase in unfolded DNA. This indirectly proved that T-ag can indeed unwind synthetic unimolecular quadruplex DNA substrates in the SPR assay conditions. Therefore, T-ag possesses quadruplex unwinding activity even though it does not contain the conserved G4 binding region present in RecQ (18), Sgs1p (19), BLM (20), and WRN (21).

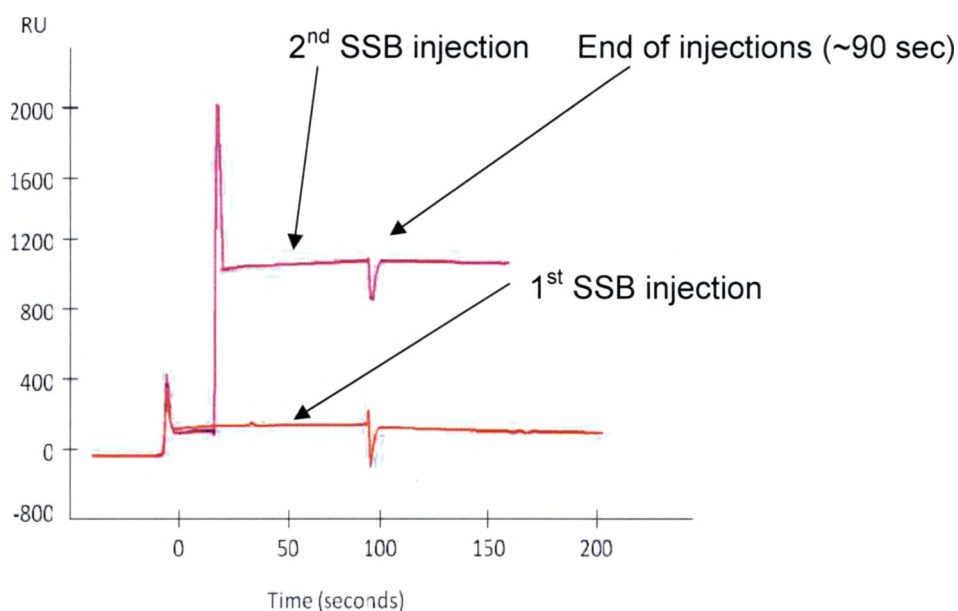


Figure 11. SSB as a reporter for G4 DNA unwinding. SSB (12 $\mu\text{g}/\mu\text{L}$, bottom trace) was injected at 30 $\mu\text{L}/\text{min}$ for 90 seconds over immobilized G4 DNA (~765 RUs), prior to injection of T-ag (13.5 nM) in HBS-EP- K^+ buffer with 10 mM Mg^{2+} at 30 $\mu\text{L}/\text{min}$ for 5 minutes (injection not shown). After the T-ag injection was complete, SSB (12 $\mu\text{g}/\mu\text{L}$) was injected a second time at 30 $\mu\text{L}/\text{min}$ for 90 seconds (top trace). The 10-fold increase in SSB binding clearly indicates that the quadruplex DNA was unwound by T-ag.

2. Double-stranded DNA experiments

The goal in these experiments was to develop a reliable assay for monitoring T-ag duplex helicase activity and its inhibition. Similar to the studies of single-stranded immobilized DNA substrates, T-ag general interactions and parameters needed to be optimized. Therefore, initially binding and unwinding events were tested, and then variable parameters were optimized. After optimization of the duplex assay conditions, a series of inhibition studies was conducted. Finally, the SV40 origin of replication sequence was incorporated

into the synthetic duplex DNA substrate to determine the effect on binding and helicase activity.

2.1 T-ag duplex helicase activity

A forked duplex was constructed with TAG DNA1 and TAG DNA2 (Table 1). The TAG DNA1 was immobilized first (~900 RUs) and then the partially complimentary TAG DNA2 was hybridized to TAG DNA1 on the chip, forming a duplex with a free 3'-tail. Interestingly, in the presence of gamma-S-ATP, T-ag could recognize and bind weakly to the forked duplex substrate but could not unwind it (Figure 12). T-ag is not expected to translocate down the DNA substrate without the energy produced from hydrolyzing ATP. A conformational change is triggered by the binding of ATP or gamma-S-ATP to T-ag, which allows for DNA binding (4), however helicase activity requires hydrolysis of the gamma phosphate of ATP. Only the T-ag in the presence of normal ATP was capable of removing the complimentary DNA strand from the immobilized TAG DNA1 (Figure 12). A corresponding drop in the baseline that is directly proportional to the amount of DNA unwound by T-ag, and thus removed from the flow cell, was observed (Figure 13). The second half of the sensorgram depicts a subsequent injection of TAG DNA2, which annealed to the TAG DNA1 that is immobilized on the surface of the sensorchip. This is the first report of T-ag helicase activity monitored by SPR-based analysis (45).

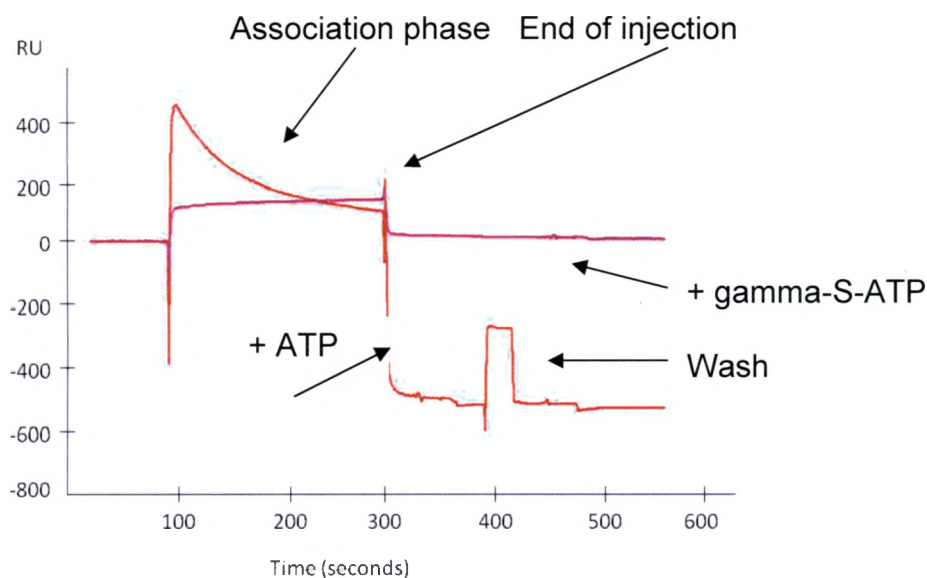


Figure 12. T-ag duplex helicase activity in the presence of ATP and gamma-S-ATP. TAG DNA1 was immobilized (~900 RUs) and hybridized to the partial complimentary TAG DNA2 *in situ* to form a forked duplex substrate. Tag (9.7 nM in HBS-EP-Mg²⁺ buffer) was injected at 20 μ L/min in the presence of 5 mM gamma-S-ATP (purple trace, 0% duplex unwound) or in the presence of 40 mM ATP (red trace, 67% duplex unwound).

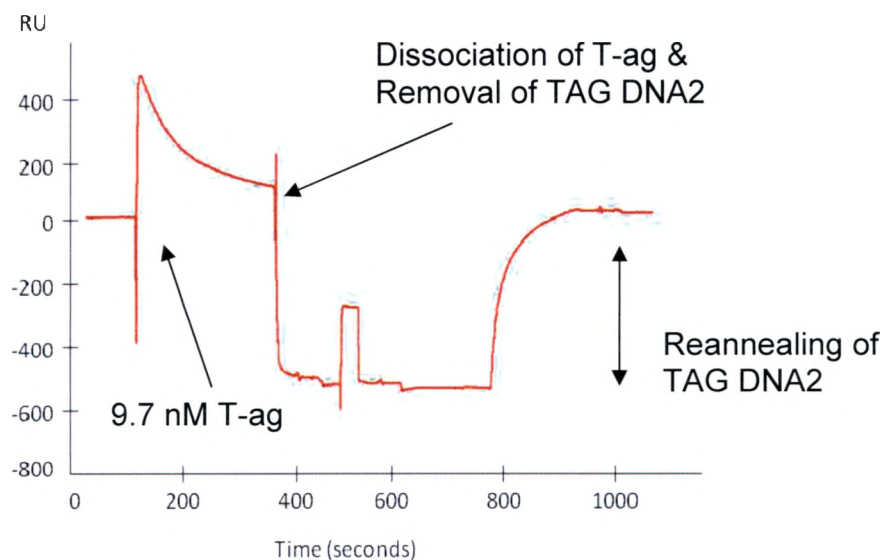


Figure 13. Duplex substrate unwinding and re-formation. The TAG DNA1/TAG DNA2 forked duplex was formed on a sensor chip as described in Figure 12. After 9.7 nM T-ag was injected at 20 μ L/min in HBS-EP-Mg²⁺ buffer in the presence of 40 mM ATP, nearly 500 RUs of DNA was removed. Finally at 800 seconds the TAG DNA2 was re-injected and the original level of hybridization was achieved.

2.2 Optimization of T-ag duplex unwinding assay

The same forked duplex substrate (TAG DNA1/TAG DNA2) was used for all of the optimization experiments. The sensor chip used in the optimization assays had ~500 RUs of TAG DNA1 immobilized, as described above, prior to duplex formation. The first parameter that was optimized was the concentration of T-ag necessary to remove nearly 100% of the TAG2 DNA from the TAG1 DNA. The normal HBS-EP- Mg^{2+} buffer was used with a constant flow rate of 20 μ L/min and 40 mM ATP per T-ag injection. A range of different T-ag concentrations was injected from 1 nM up to 14 nM. It was determined that the concentration of 2.9 nM T-ag removed approximately 90% (a target percentage that is still measurable) of the TAG DNA2, leaving just TAG DNA1 in the single-stranded state (Figure 16). Also, it was noted that the SPR curve didn't display any rebinding of free T-ag after the initial binding and unwinding activity. The optimized concentration of T-ag (2.9 nM) was used in all of the remaining optimization assays.

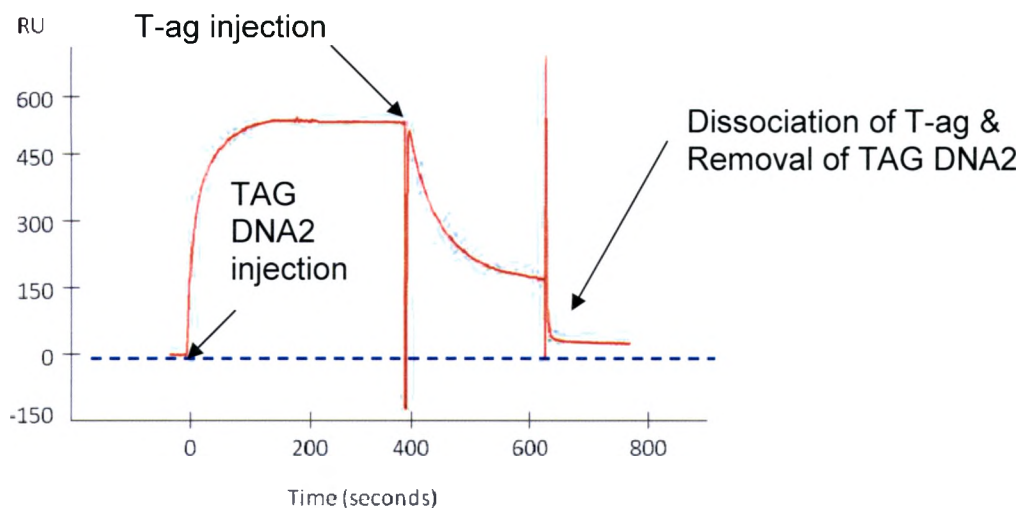


Figure 14. Determination of T-ag concentration to remove ~90% of complimentary duplex strand (TAG DNA2). The TAG DNA1/TAG DNA2 forked duplex was formed on a sensor chip as described in Figure 12. After 2.9 nM T-ag was injected at 20 $\mu\text{L}/\text{min}$ in HBS-EP- Mg^{2+} buffer in the presence of 40 mM ATP, nearly 500 RUs of DNA was removed. Based on equation 5 (Chapter II) 91% of the DNA substrate was unwound. Therefore, this concentration of T-ag was used in subsequent optimization assays.

The effect of varying the NaCl concentration in the running buffer and injection samples was also determined. The running buffer in previous assays was HBS-EP- Mg^{2+} Buffer (0.01 M HEPES, pH 7.4, 0.15 M NaCl, 10 mM MgCl_2 , 3 mM EDTA, and 0.005% v/v P20 surfactant). The amount of NaCl was varied from 1.5 mM to 300 mM in the HPS-EP- Mg^{2+} Buffer and all other parameters were kept constant, including the ATP concentration (40 mM ATP) in the T-ag injection samples. T-ag was observed to possess duplex helicase activity at each NaCl concentration tested. The % unwound was calculated for each individual salt assay using equations 3-5. It was determined that at the lowest salt concentration, 1.5 mM, T-ag unwound 96% of the forked duplex substrate

available. Conversely, at the highest salt concentration, 300 mM, T-ag only unwound 86% of the forked substrate. Increased ionic strength was detrimental to T-ag helicase activity (Figure 15).

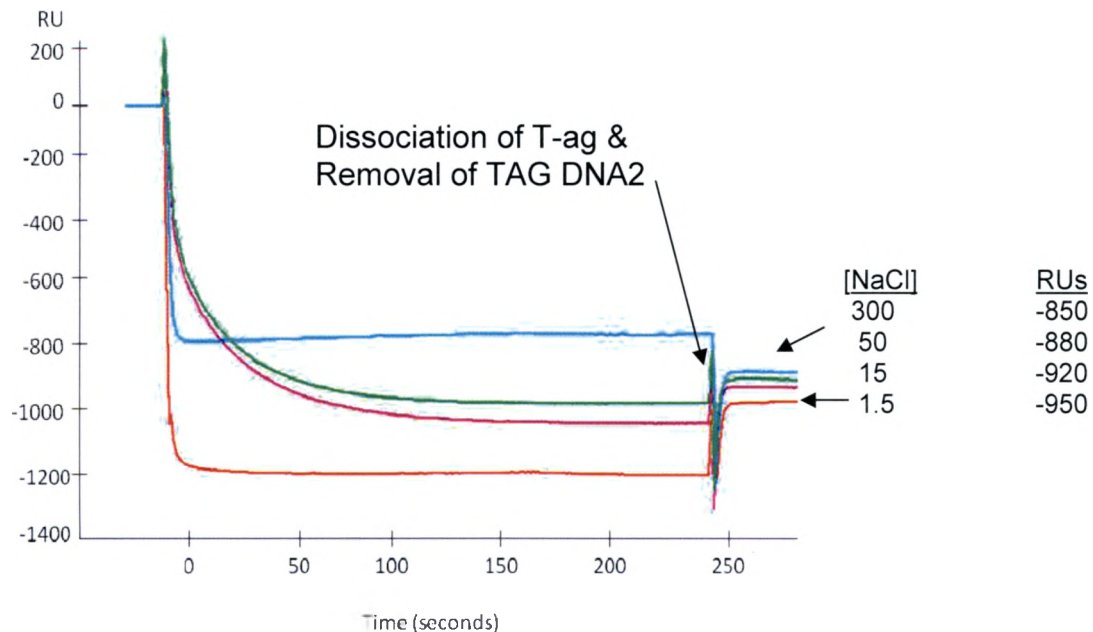


Figure 15. Salt optimization assay for T-ag duplex helicase activity. The forked duplex substrate (TAG DNA1/TAG DNA2) was formed on the sensor chip as in Figure 12, and 2.9 nM of T-ag was injected at 20 $\mu\text{L}/\text{min}$ with 40 mM ATP in HBS-EP- Mg^{2+} buffer with varying NaCl concentration: 1.5 mM (red trace), 15 mM (magenta trace), 50 mM (green trace), and 300 mM (light blue trace). T-ag in the 1.5 mM NaCl-containing buffer removed the highest percent of TAG DNA2, 96%, whereas in the presence of 300 mM NaCl the least amount of TAG DNA2, 86%, was removed.

Finally, the contact time between T-ag and DNA substrate required for optimal unwinding activity was determined. The volume of T-ag injected over the forked duplex substrate was varied (8.0, 17.0, 42.0, 67.0, and 75.0 μL , respectively). The observed result was that equal amounts of DNA were removed for T-ag contact times of 25, 50, 125, and 200 seconds (Figure 16 and

Table 2). Under the SPR assay conditions T-ag helicase activity was virtually instantaneous, with the same amount of the partially complimentary DNA strand removed at both 20 seconds and 200 seconds (Figure 16). This was an important phase of the optimization assays because it allowed the use of even smaller injection sizes than used in previous assays, which helped to conserve costly enzyme supplies and other reagents. Results for optimization of buffer ionic strength and contact time are tabulated in Table 2.

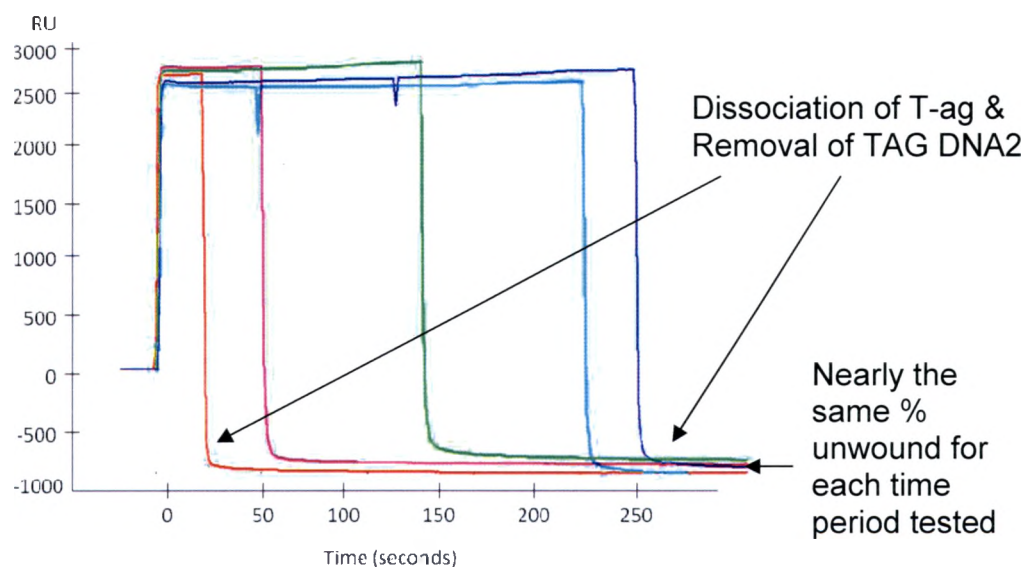


Figure 16. Optimal contact time for T-ag helicase activity. The TAG DNA1/TAG DNA2 forked duplex was formed on a sensor chip as described in Figure 12. At a flow rate of 20 $\mu\text{l}/\text{min}$ injection volumes for five various contact times were calculated (red trace = 25 sec, magenta trace = 50 sec, green trace = 125 sec, light blue trace = 200 sec, and dark blue trace = 225 sec, respectively). It was determined that nearly the same amount of DNA was unwound regardless of contact time. However, longer injection times seemed to allow for a small amount of T-ag rebinding. Data shown are for the DNA-containing flowcell only and is not reference-subtracted.

Contact Time (sec)	NaCl (mM)	% unwound
300	1.5	96
300	15	91
300	50	89
300	300	86
25	1.5	97
50	1.5	90
125	1.5	97
200	1.5	97
225	1.5	82

Table 2. Summary of contact time and salt optimization assays. The percent DNA unwound was calculated using equations 3-5 to determine the relative helicase activity of T-ag under the various conditions. The % unwound decreased as the NaCl concentration was increased, and conversely remained nearly constant regardless of contact time. It should be noted that at 50 and 225 seconds the slight decrease in % unwound is likely due to T-ag rebinding after the initial unwinding event.

2.3 Inhibition of T-ag duplex helicase activity

The ability to determine T-ag duplex helicase inhibition by three known DNA-interactive small molecules, TMPyP4, Distamycin A, and Tel 11, using SPR was assessed. Inhibition of T-ag duplex helicase activity was tested first using the known T-ag inhibitor TMPyP4 (33), and was observed in real-time (Figure 17). TMPyP4 at various concentrations was injected in the manual inject mode just prior to injection of T-ag, ATP, and Mg^{2+} . The percent unwound of forked duplex substrate decreased with increasing concentration of TMPyP4 added prior to T-ag injection. It is noteworthy that inhibition of unwinding *only* occurred when TMPyP4 was added to the DNA substrate *prior* to injection of T-ag. When TMPyP4 was premixed with T-ag, ATP, and Mg^{2+} before all were injected simultaneously, duplex unwinding proceeded as usual (data not shown). This implies that TMPyP4 does not inhibit SV40 T-ag through a direct interaction with

the hexameric helicase but rather through an interaction with the T-ag/DNA complex. TMPyP4 must already be associated with the DNA substrate for inhibition to occur.

After testing the known T-ag inhibitor, TMPyP4, the assays were repeated as described above using Distamycin A (Figure 18) and Tel 11 (Figure 19) in place of TMPyP4. As described both Distamycin A and Tel 11 both can bind to duplex DNA (22, 36, 39, and 40), although Tel 11 binds to a lesser extent. Therefore, all three small molecules should be able to bind to the duplex DNA substrate before injecting T-ag, thereby inhibiting the helicase activity. A significant advantage of using SPR to investigate these interactions is the ability to observe the individual interactions in real-time, as opposed to evaluating the end result only. This allows analysis of the sequence of events required for effective inhibition.

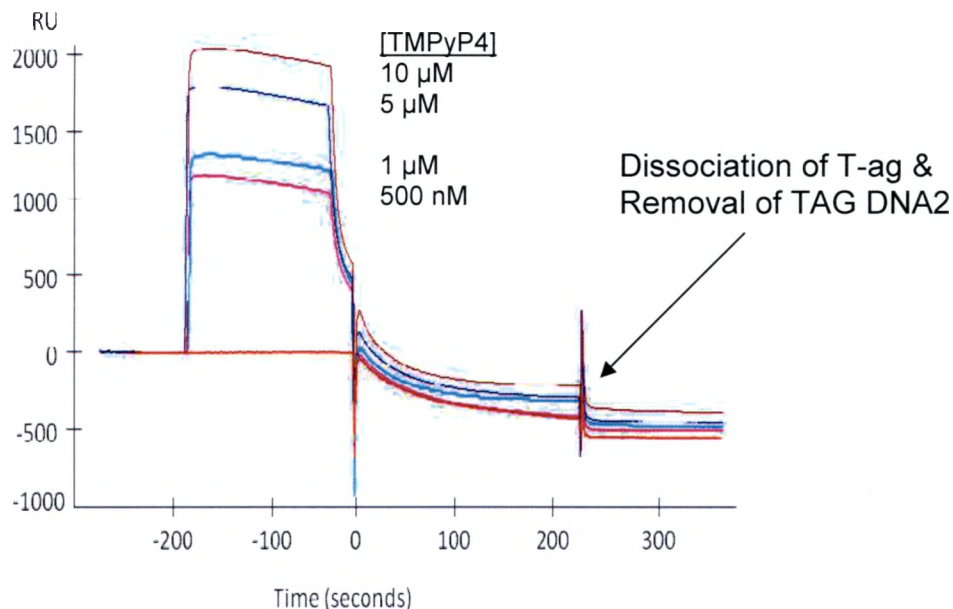


Figure 17. TMPyP4 inhibition of T-ag duplex helicase activity. The TAG DNA1/TAG DNA2 forked duplex was formed on a sensor chip as described in Figure 12. Prior to injecting 9.7 nM of T-ag with 40 mM ATP in HBS-EP-Mg²⁺ Buffer at 20 μ L/min, a 70 μ l injection of TMPyP4 was injected. The concentrations of TMPyP4 were 0 nM (red trace), 500 nM (magenta trace), 1 μ M (light blue trace), 5 μ M (dark blue trace), and 10 μ M (brown trace) respectively. After each injection of T-ag, TAG DNA2 was rehybridized to form the duplex substrate. For this assay ~500 -600 RUs of TAG DNA1 was initially immobilized on the sensor chip.

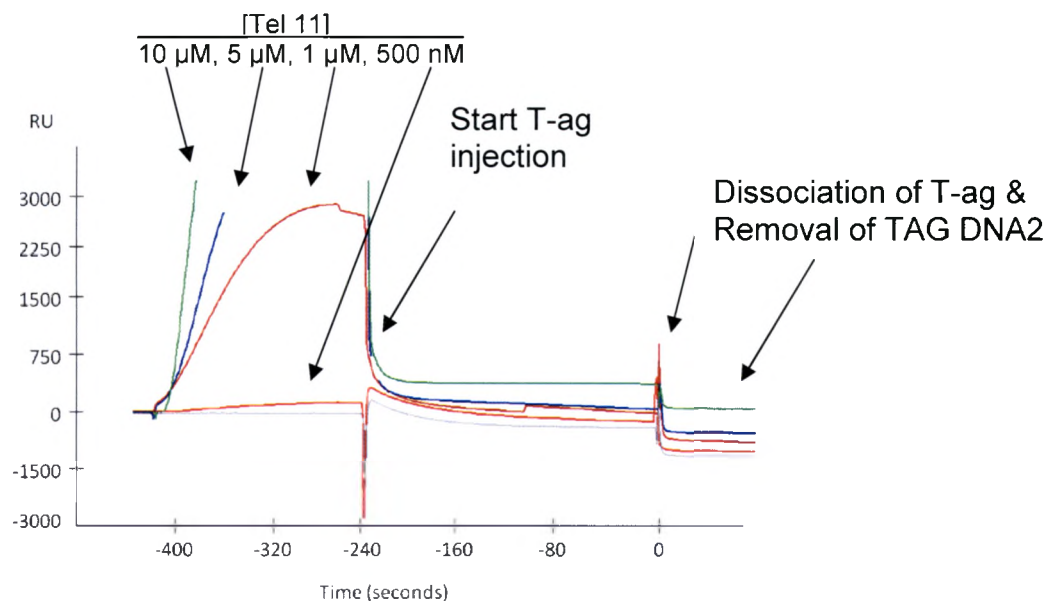


Figure 18. Tel 11 inhibition of T-ag duplex helicase activity. The TAG DNA1/TAG DNA2 forked duplex was formed on a sensor chip as described in Figure 12. Prior to injecting 9.7 nM of T-ag with 40 mM ATP HBS-EP-Mg²⁺ Buffer at 20 μ L/min, a 70 μ L injection of Tel 11 was injected. The concentrations of Tel 11 were 0 nM (magenta trace), 500 nM (red trace), 1 μ M (brown trace), 5 μ M (dark blue trace), and 10 μ M (green trace) respectively. After each injection of T-ag, TAG DNA2 was rehybridized to form the duplex. For this assay ~ 500 - 600 RUs of TAG DNA1 was initially immobilized on the sensor chip. This sensorgram was re-sized (cropping the response for higher concentrations of Tel 11) using the Biaevaluation software to more clearly show the extent of T-ag inhibition.

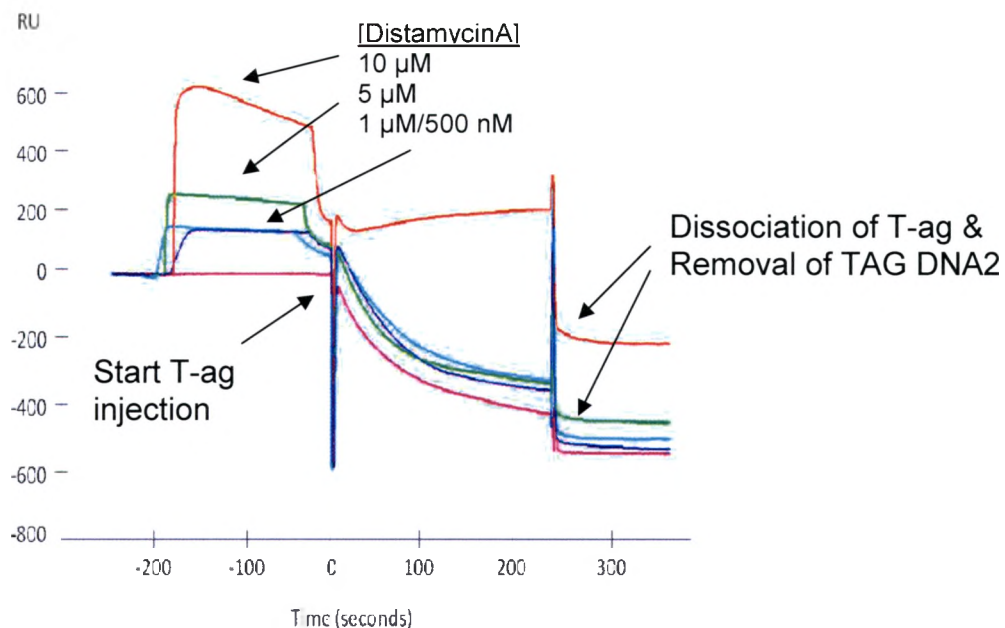


Figure 19. Distamycin A inhibition of T-ag duplex helicase activity. The TAG DNA1/TAG DNA2 forked duplex was formed on a sensor chip as described in Figure 12. Prior to injecting 9.7 nM of T-ag with 40 mM ATP HBS-EP-Mg²⁺ Buffer at 20 μL/min, a 70 μl injection of Distamycin A was injected. The concentrations of Distamycin A were 0 nM (magenta trace), 500 nM (dark blue trace), 1 μM (light blue trace), 5 μM (green trace), and 10 μM (red trace) respectively. After each injection of T-ag, TAG DNA2 was rehybridized to form the duplex. For this assay ~500 -600 RUs of TAG DNA1 was initially immobilized on the sensor chip.

TMPyP4 (Figure 17), Tel11 (Figure 18), and Distamycin A (Figure 19) all inhibited the unwinding of the duplex DNA by T-ag. At 10 μM concentrations the percent of the DNA unwound was decreased on average to 53%, 47%, and 30% respectively, making Distamycin A the most potent inhibitor in these initial assays (Table 3). The extent of T-ag duplex helicase inhibition observed by Tel 11 was somewhat surprising, since the equilibrium binding constant of the Tel 11/duplex DNA interaction is ~60 μM compared to ~5 μM for the binding of TMPyP4 to duplex DNA (17). However the stoichiometry of Tel 11 binding is much higher

and this may lead to the observed inhibition. The sensorgrams shown in each figure are one representative assay from the group of total experiments performed.

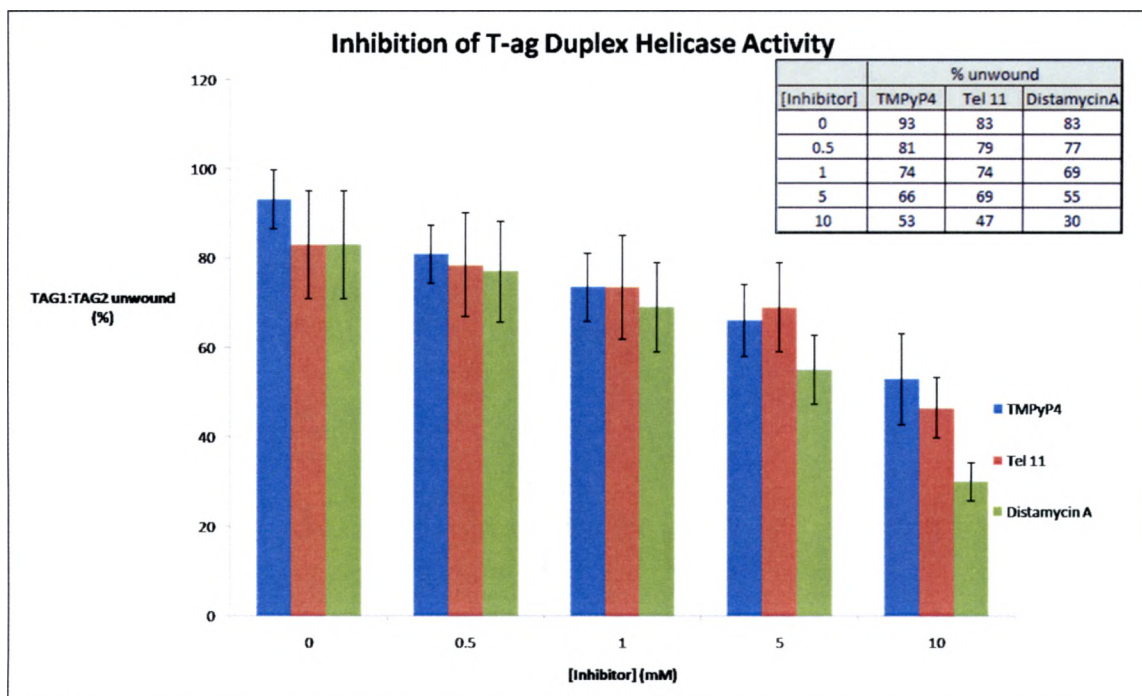


Table 3. Inhibition of T-ag duplex helicase activity by TMPyP4, Tel11, and Distamycin. The TAG DNA1/TAG DNA2 forked duplex was formed on a sensor chip as described in Figure 12. In each case the inhibitor (0 mM to 10 mM) was injected prior to T-ag (9.7 nM) injections. The % unwound of duplex DNA was calculated using equations 3-5 (Chapter II). The data shown here are based on the average from all inhibition assays performed. The inset chart shows the raw numerical data for one determination.

2.4 T-ag binding to OR-containing DNA substrates

In order to investigate the effect of sequence context on T-ag binding and helicase activity observed in this SPR-based assay, DNA substrates containing a portion of the SV40 OR were constructed. T-ag displayed an increased binding affinity to a synthetic DNA substrate containing the complete SV40 origin of

replication sequence (TAG-OBDD *versus* the random nucleotide substrates utilized earlier). In fact the T-ag bound very tightly with the DNA and could only be removed with difficulty, but no unwinding of any kind was displayed (Figure 20). All parameters were identical to the initial duplex unwinding assays, except for the sequence and length of the synthetic DNA substrate. This DNA substrate was longer and possessed a much higher T_m than the previously used forked duplex substrates. The high T_m of the TAG-OBDD and the palindromic nature of the sequence made hybridization of the complementary strands difficult to accomplish on the sensor chip. Partial hybridization (~50%) was achieved at elevated temperature; however, the Biacore X can only be heated to 40 °C in the flowcell, which was insufficient for complete hybridization. It is likely that the TAG-OBDD sequence easily forms a self-contained hairpin structure, further complicating the hybridization of the desired complementary sequence.

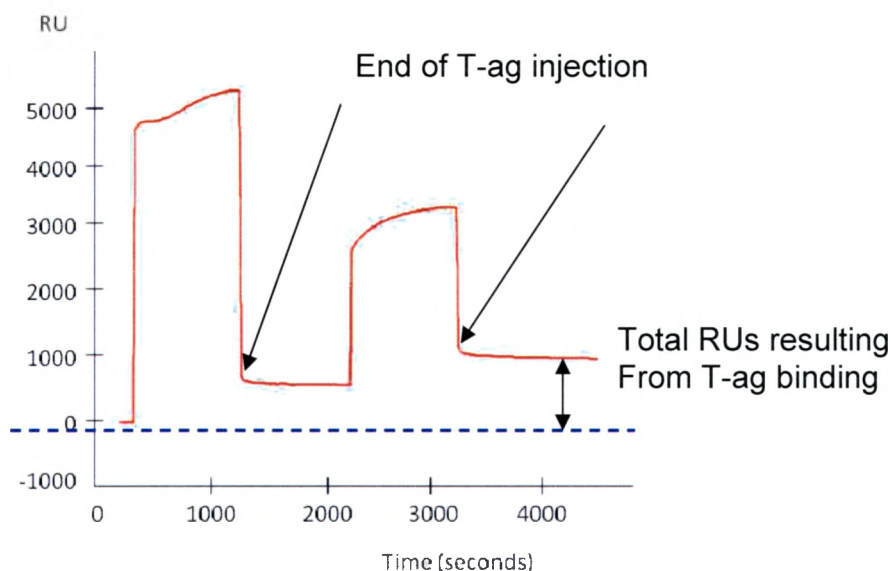


Figure 20. T-ag binding to the SV40 origin of replication sequence. TAG-OBD (~500 RUs) was immobilized on the SA sensor chip and hybridized to Fragment C (~200 RUs) on the chip. Complete hybridization could not be achieved, presumably due to the propensity of the TAG-OBD sequence to form a self-contained hairpin structure. Two injections of T-ag (first = 9.7 nM at time 0, second = 4.5 nM at time 2200 seconds) with ATP and Mg^{2+} were performed but the OR-containing sequence was not unwound by the T-ag. The increased recognition and binding of T-ag rendered the T-ag/DNA complex stable to dissociation and no loss of RU during the dissociation phase of the injections was observed. The data shown are from the DNA-containing flowcell only and are not reference-subtracted.

A shorter DNA substrate (ODNA) was obtained that only contained a partial site II region (three of the four pentanucleotide palindromes) and lacking the AT rich region. Complete hybridization of this sequence with its complement was achieved on the sensor chip. T-ag was observed to show an increased binding affinity to the ODNA duplex substrate as well and no unwinding was displayed (Figure 21). The total amount of T-ag bound was much higher for the complete OR-containing substrate, TAG-OBD:Fragment C (~1000 RUs)

compared to the partial OR-containing substrate, ODNA: ODNComp2 (~250 RUs), however. Both of these OR-containing substrates contained a short 3'-free end and we had anticipated that unwinding would occur. However, the increased T_m of the DNA substrates may render them much more stable to unwinding by the T-ag hexamer under the SPR-based assay conditions. Alternatively, re-hybridization of the duplex may occur quickly even in the event of minor unwinding, especially in the absence of single-stranded binding proteins. The effect of longer T-ag/DNA contact time, altered buffer conditions, and additional accessory proteins have not been tested in this case.

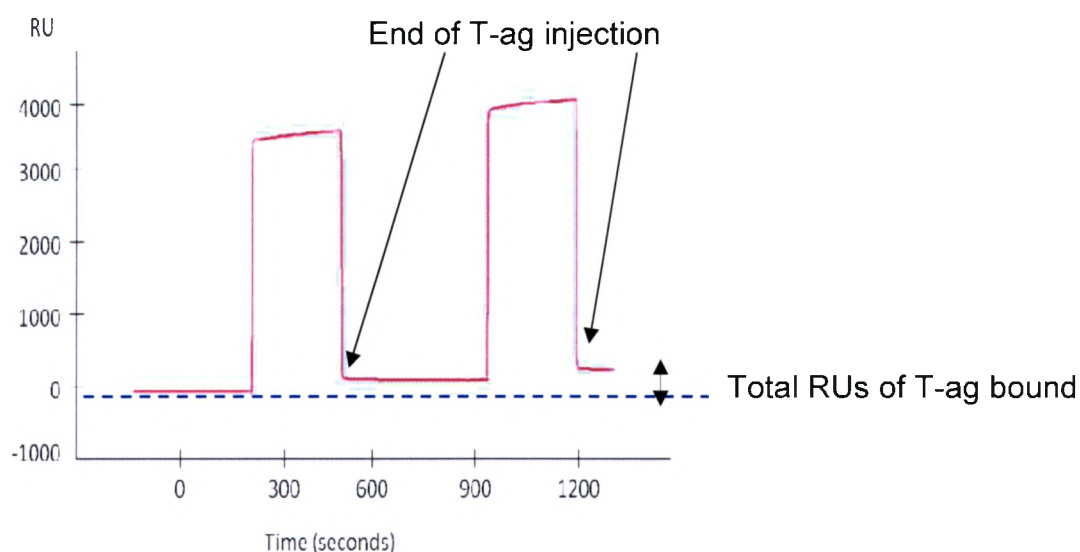


Figure 21. T-ag binding to the partial SV40 origin of replication sequence. Two injections of T-ag (9.7 nM) with ATP and Mg^{2+} were performed over the ODNA:ODNComp2 (~275 RUs of each) duplex on the sensor chip surface. The partial origin of replication containing sequence was not unwound by the T-ag, but the increased recognition and binding of T-ag allowed the protein to stay bound to the DNA after the end of the injection. Thus, there was no loss of RU during the dissociation phase of the injections.

The results obtained from the two OR containing DNA assays both correspond to previous research showing that T-ag has an increased affinity for

the OR sequence (11). Also, this affinity is not completely diminished when portions of the OR sequence are removed. This was shown by SPR when the sequence was shortened and the same binding results were observed.

Therefore, T-ag doesn't require the entire OR sequence in order to recognize and bind the origin of replication with high affinity.

3. Improved intramolecular G-quadruplex DNA unwinding experiments

In order to monitor the unwinding of an intramolecular quadruplex DNA substrate without the use of any secondary reporters, we used the strategy outlined in Figure 7 (Chapter I). TAG DNA1 was immobilized on a SA chip and then partially complementary TAGcompG4 was hybridized to the immobilized single-stranded oligonucleotide in HBS-EP-K⁺ buffer. The 3'-tail region of the complement contained the human telomeric repeat 5'-(TTA GGG)₄-3', capable of forming an intramolecular quadruplex region in the presence of potassium ion. In order to unwind the partial duplex region of the DNA substrate, T-ag would first need to unwind and translocate through the intramolecular quadruplex-forming region of the substrate. Under the correct buffer conditions, a loss of complementary DNA from the chip would thus represent intramolecular quadruplex helicase activity.

The interaction between T-ag and the TAG DNA1/TAGcompG4 DNA substrate was greatly reduced when gamma-S-ATP (a non-hydrolyzable ATP analog) was used in place of ATP (Figure 22). The T-ag hexamer should not be able to translocate in the presence of gamma-S-ATP so the observed response represents binding of the hexamer to the DNA, but not translocation. When ATP

was available, the observed binding response was much higher. It is therefore reasonable to assume that in the presence of ATP multiple T-ag hexamers load onto the same DNA substrate as translocation proceeds and T-ag unwinds the G-quartet region before unwinding the duplex region responsible for tethering the complementary DNA to the sensor chip. The G-quadruplex helicase activity was reflected in the significant drop in RUs in the presence of ATP, after dissociation of T-ag. This repeated loading would be greatly diminished in the presence of gamma-S-ATP, in accordance with the observed response.

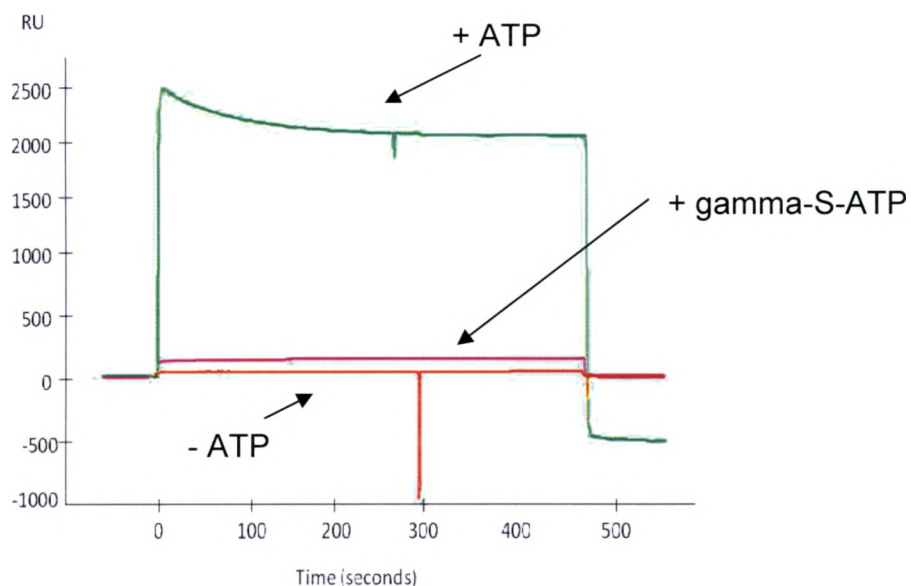


Figure 22. T-ag binding to TAG DNA1/TAGcompG4 complex without ATP, in the presence of gamma-S-ATP, and with ATP. T-ag (2.3 nM) was injected at 10 $\mu\text{L}/\text{min}$ in HBS-EP- Mg^{2+} buffer in the absence of ATP (red trace), presence of 5 mM gamma-S-ATP (purple trace), and presence of 40 mM ATP (green trace). Although a higher concentration of ATP was used compared to gamma-S-ATP, the observed response is 25-fold *higher* in the presence of ATP. In addition, *no* loss of complementary DNA from the chip is observed in the absence of ATP. The amount of TAG DNA1 immobilized was ~ 800 RUs and the sensorgrams are from the DNA-containing flowcell only, representing absolute response (RUs).

Furthermore, the drop in RUs observed in response to T-ag injection over the TAG DNA1/TAGcompG4 DNA substrate in the presence of ATP was reproducible (Figure 23) and could be exactly compensated for by rehybridization of the complement to the chip (data not shown), as in the case for unwinding of duplex substrates. This is the first direct real-time demonstration of T-ag quadruplex helicase activity using SPR.

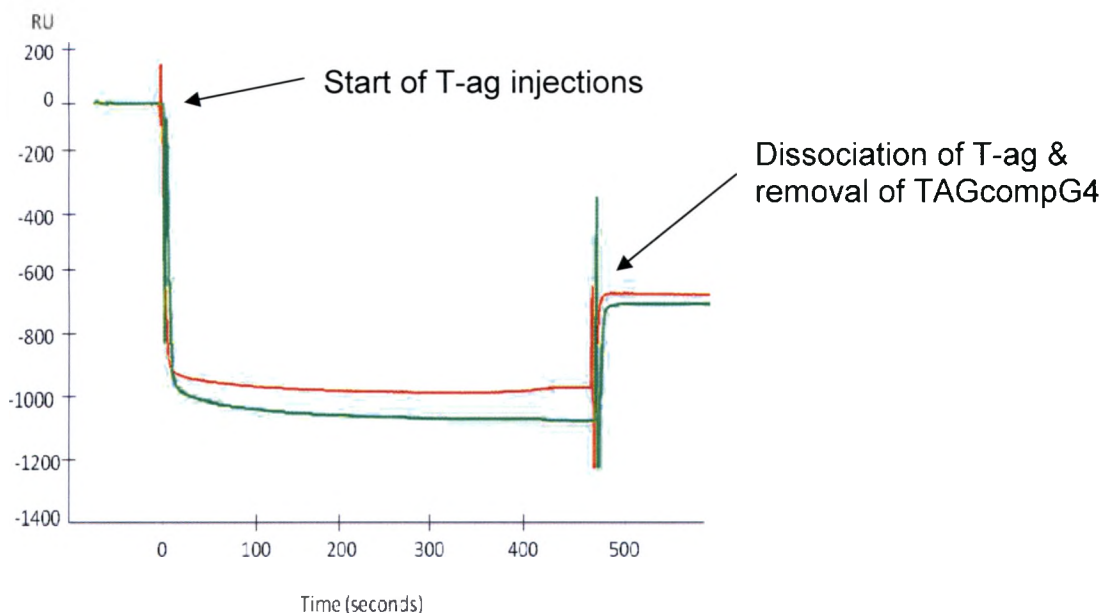


Figure 23. T-ag binding and unwinding of TAG1:TAGcompG4. Two identical injections of 2.3 nM T-ag at 10 $\mu\text{L}/\text{min}$ containing 40 mM ATP and 10 mM Mg^{2+} were performed on the G4' containing substrate (~ 1000 RUs TAG DNA1 immobilized). The running buffer containing 150 mM KCl was flowed over the DNA substrate for 3000 sec prior to T-ag injections in Mg^{2+} -containing buffer to allow for the folding of the intramolecular quadruplex region. Successful T-ag helicase activity to unwind the quadruplex region and the duplex region of the DNA substrate (removal of 80-83% of the TAGcompG4 from the sensor chip surface) was reproducible.

4. Summary of Results

T-ag was shown to bind single-stranded, double-stranded, and quadruplex DNA substrates using SPR-based analysis. Helicase activity was ATP-dependent and occurred in the directional manner reported for T-ag.

Optimization of the SPR-based duplex unwinding assay was performed and the inhibition of T-ag duplex helicase activity was investigated using three small DNA interactive agents: TMPyP4, Tel 11, and Distamycin A. All three small molecules were observed to inhibit T-ag duplex helicase activity under these

conditions. An improved SPR intramolecular quadruplex unwinding assay was developed. The improved quadruplex unwinding assay may now be used for future studies, in which potential G-quadruplex stabilizing small molecules can be tested for inhibition. If these small molecules do in fact stabilize the G-quadruplex structures and thereby inhibit quadruplex unwinding, they could potentially possess anti-cancer or other therapeutic properties.

Formation of an intramolecular quadruplex DNA substrate was demonstrated using SSB for the immobilized human telomeric repeat. However, formation of the intramolecular quadruplex forming region of the DNA substrate in the improved quadruplex unwinding assay was only inferred by using appropriate conditions for quadruplex formation. Formation of this quadruplex forming region *on the sensor chip* will be verified in the near future by demonstrating a lack of binding to a duplex complementary oligonucleotide for the quadruplex repeat sequence.

Ultimately, extension of this real-time SPR assay of helicase activity and inhibition to other quadruplex-processing enzymes will hopefully enlarge the current knowledge concerning helicase function.

APPENDIX

David Lab Protocol 001
DNA
Jason R Plyler

Salt Optimization Assay with T-ag/ Duplex

November 21, 2008

1. Acquire a Sensor SA with ~250-500 RUs of TAG DNA 1 immobilized on flowcell 2.
2. Prepare a 1:100 dilution of fresh TAG DNA 2 in HBS-EP buffer.
3. Filter and degas five different HBS-EP buffers with varying NaCl concentrations.
 - a. 1.5 mM NaCl
 - b. 15 mM NaCl
 - c. 50 mM NaCl
 - d. 150 mM NaCl
 - e. 300 mM NaCl
4. Weigh five 6 mg, small fractions of ATP powder from the -20°C freezer.
 - a. Dissolve each separate ATP fraction in 130 μ L of the running buffers prepared in #3
5. Pull the dilution stock of T-ag out of the -20°C freezer and put on dry-ice for future use.
6. Take the Biacore Instrument out of continuous mode
 - a. Put the buffer loop into the correct buffer (a-e from #3), Prime twice
 - b. Begin a sensorgram use multichannel mode and choose FC1 as the reference
 - c. Select 20 μ L/ min as a flowrate
 - d. Check to see that baseline is reasonable (~20,000 RU s, not 90,000!)
7. Go to command: inject and change volume to 50ul with a delayed wash of 60 sec
 - a. Pipette 70 μ L of the TAG2 solution, followed by 5 μ L air, 5 μ L sample, 5 μ L air
 - b. Load the sample and click inject
 - c. Flag the injection point for future reference
8. Prepare the T-ag injection sample in sterile eppendorff tube (Wearing gloves!)
 - a. Add 64 μ L of the current running buffer
 - b. Add 1 μ L of the diluted T-ag from dry-ice container
 - c. Lastly, add 65 μ L of the correct ATP mixture from #4

- d Vortex this 130 μL sample
- 9. Go to command: inject and change the volume to 80 μL with a delayed wash of 300 sec
 - a. Pipette 100 μL of the sample from #8, followed by 5 μL air, 5 μL sample, 5 μL air
 - b. Load the sample and click inject
 - c. Flag the injection point for future reference
- 10. Go to command: inject and change volume to 20 μL with a normal wash
 - a. obtain Karl's regeneration solution
 - b. filter before use with a small syringe with a filter
 - c. Pipette 40 μL , followed by 5 μL air, 5 μL sample, 5 μL air
 - d. Flag the injection point for future reference
- 11. Repeat steps 7-10, before stopping the sensorgram and changing to the next running buffer and re-priming the system.
- 12. Store everything and clean up, check sterile tips and tubes for the next student.

David Lab Protocol 002
Jason R Plyler

Protocol for HBS-EP Buffer
November 31, 2008

Standard Concentrations:

10 mM HEPES, 3 mM EDTA, 150 mM NaCl, 0.005%(v/v) P20, at pH 7.4.

Raw Materials Needed:

- HEPES Buffer powder FW: 260.29 g/mol
- EDTA chelating agent FW: 372.24 g/mol
- MgCl₂ FW: 203.3 g/mol
- NaCl FW: 58.44 g/mol
- KCl FW: 74.56 g/mol

For 1 Liter of Standard Buffer Solution:

1. Obtain an autoclaved, clean 1 liter screw-top bottle, and fill with 800 mL of diH₂O.
2. Weigh out the correct masses of each raw material and pour into the 800 mL of diH₂O
 - a. 2.60 g HEPES
 - b. 1.1 g EDTA
 - c. 8.766 g NaCl
3. Add diH₂O up to the 1 liter mark, then pipette in 50 μ L of P20
4. Check the pH, and adjust to 7.4 using NaOH or HCl solutions as needed.
5. Filter with 20 micron filter prior to use, leaving on vacuum for 10 minutes to degas.

For Mg²⁺ containing buffer simply add 2.0 g of MgCl₂ to the above three materials prior to filling with diH₂O to the 1 liter mark.

When working with G-quartet containing DNA, use ONLY KCl as your salt in the buffer. For a 150 mM K⁺ HBS-EP Buffer follow the protocol above, but substitute the following in step 2:

- a. 2.60 g HEPES
- b. 1.1 g EDTA
- c. 11.2 g KCl

Then proceed to steps 3-5 as above.

REFERENCES

1. Wang, W., Manna, D., and Simmons, D.T. (2007) *J. Virol.*, **81**, 4510-4519.
2. Tijan, R. (1978) *Cell*, **13**, 165-179.
3. Flint, S.J., Racaniello, V.R., Enquist, L.W., Skalka, A.M., and Krug, R.M. (2000) *Principles of Virology: Molecular Biology, Pathogenesis, and Control*, ASM Press, Washington, DC.
4. Stahl, H., Droge, P., and Knippers, R. (1986) *EMBO J.*, **5**, 1939-1944.
5. Deb, S., Delucia, A.L., Koff, A., Tsui, S., and Tegtmeyer, P. (1986) *Mol. Cell. Biol.*, **6**, 4578-4584.
6. Dean, F.B., Borowiec, J.A., Eki, T., and Hurwitz, J. (1992) *J. Biol. Chem.*, **267**, 14129-14137.
7. Borowiec, J.A., Dean, F.B., Bullock, P.A. and Hurwitz, J. (1990) *Cell*, **60**, 181-184.
8. Mastrangelo, I.A., Hough, P.V.C., Wall, J.S., Dodson, M., Dean, F.B., and Hurwitz, J. (1989) *Nature (London)*, **338**, 658-662.
9. Gai, D., Li, D., Finkielstein, C., Ott, R., Taneja, P., Fanning, E., and Chen, X., (2004) *The Journal of Biological Chemistry*, **37**, 38952-38959.
10. Sullivan, C.S., and Pipas, J.M. (2002) *Microbiol. Mol. Biol. Rev.*, **66**, 179-202.
11. Bullock, P.A. (1997) *Crit. Rev. Biochem. Mol. Biol.*, **32**, 503-568.
12. Li, D., Zhao, R., Lilyestrom, W., Gai, D., Zhang, R., DeCaprio, J., Fanning, E., Jochimiak, A., Szakonyi, G., and Chem, X. (2003) *Nature*, **423**, 512-518.
13. Hanson, P.I., and Whiteheart, S.W. (2005) *Nat. Rev. Mol. Cell Biol.*, **6**, 519.
14. Fanning, E., and Knippers, R. (1992) *Annu. Rev. Biochem.*, **61**, 55-85.
15. SenGupta, D.J., and Borowiec, J.A. (1992) *Science*, **256**.
16. Baran, N., Pucshansky, L., Marco, Y., Benjamin, S., and Manor, H. (1997) *Nucl. Acids Res.*, **25**, 297-303.
17. Tuesuwan, B., Kern J.T., Thomas P.W., Rodriguez M., Li J., David W.M., and Kerwin, S.M. (2008) *Biochem.*, **47**, 1896-1909.
18. Wu, X., and Maizels, N. (2001) *Nucl. Acids Res.*, **29**, 1765-1771.
19. Sun, H., Bennett, R.J., and Maizels, N. (1999) *Nucl. Acids Res.*, **27**, 1978-1984.
20. Sun, H., Karow, J.K., Hickson, I.D., and Maizels, N. (1998) *J. Biol. Chem.*, **273**, 27587-27592.
21. Fry, M., and Loeb, L.A. (1999) *J. Biol. Chem.*, **274**, 12797-12802.
22. Gupta, R., and Brosh, R.M., Jr. (2007) *Curr. Med. Chem.*, **14**, 503-517.

23. Hickson, I.D. (2003) *Nat. Rev. Cancer*, **3**, 169-178.
24. Hubbert, J.L., and Balasubramanian, S. (2005) *Nucleic Acids Res.*, **33**, 2908-2916.
25. Duquette, M.L., Handa, P., Vincent, J.A., Taylor, A.F., and Maizels, N. *Genes Dev.* 2004, **18**, 1618.
26. Evans, T., Schon, E., Gora-Maslak, G., Patterson, J. and Efstratiadis, A. (1984) *Nucleic Acids Res.*, **12**, 8043-8058.
27. Shimizu, A. and Honjo, T. (1984) *Cell*, **36**, 801-803.
28. Wu, Y., Shin-ya, K., and Brosh, R.M., Jr. (2008) *Mol. Cell. Biol.* **28**, 4116-4128.
29. Simmons, D.T. (2000) *Advances in Virus Research*, **55**, 75-134.
30. Blackburn, E.H. (1994) *Cell*, **77**, 621-623.
31. Weinrich, S.L., Pruzan, R., Ma, L., Ouellette, M., Tesmer, V.M., Holt, S.E., Bodnar, A.G., Lichtsteiner, S., Kim, N.W., and Trager, J.B. (1997) *Nat. Genet.*, **17**, 498-502.
32. Gowan, S.M., Harrison, J.R., Patterson, L., Valenti, M., Read, M.A., Neidle, S., and Kelland, L.R. (2002) *Mol. Pharm.*, **61** (5), 1154-1162.
33. Duquette, M.L., Huber, M.D., and Maizels, N. (2007) *Cancer Res.*, **67**, 2586-2594.
34. Tian-miao O., Yu-jing L., Jia-heng T., Zhi-shu H., Kwok-Yin W., Lian-quan G. (2007) *J. Med. Chem.*, **50** (7), 1465 -147.
35. Wheelhouse, R.T., Han, D.S.H., Han, F.X., and Hurley, L.H. (1998) *J. Am. Chem. Soc.*, **120** (13) 3261-3262.
36. Huber, M.D., Lee, D.C. and Maizels, N. (2002) *Nucleic Acids Res.*, **30**, 3954-3961.
37. Li, J.L., Harrison, R.J., Reszka, A.P., Brosh, R.M., Bohr, V.A., Neidle, S., and Hickson, I.D. (2001) *Biochemistry*, **40**, 15194-15202.
38. Han, H., Langley, D.R., Rangan, A., and Hurley, L.H. (2001) *J. Am. Chem. Soc.*, **123**, 8902-8913.
39. David, W.M., Brodbelt, J., Kerwin, S.M., and Thomas, P.W. (2002) *Anal. Chem.*, **74**, 2029-2033.
40. Randazzo, A., Galeone, A., and Mayol, L. (2001) *Chem. Commun.*, **11**, 1030-1031.
41. Cocco, M.J., Hanakahi, L.A., Huber, M.D. and Maizels, N. (2003) *Nucleic Acids Res.*, **31**, 2944-2951.
42. Rasnik, I., Myong, S., and Ha, T. (2006) *Nucleic Acids Res.*, **34** (15), 4225-4231.
43. Wilson, W.D. (2002) *Science* **295**, 2103-2104.
44. Gitlin, G., Bayer, E.A., and Wilchek, M. (1987) *J. Biochem.*, **242**, 923-926.
45. Plyler, J., Jasheway, K., Tuesuwan, B., Karr, J., Brennan, J.S., Kerwin, S.M., and David, W.M. (2009) *Cell Biochem. Biophysics* **53**, 43-52.

